

## Seismic stratigraphy of the Central Basin in northwestern Ross Sea slope and rise, Antarctica: Clues to the late Cenozoic ice-sheet dynamics and bottom-current activity

Sookwan Kim<sup>a,b</sup>, Laura De Santis<sup>c</sup>, Jong Kuk Hong<sup>a,b,\*</sup>, Diego Cottlerle<sup>c</sup>, Lorenzo Petronio<sup>c</sup>, Ester Colizza<sup>d</sup>, Young-Gyun Kim<sup>a,e</sup>, Seung-Goo Kang<sup>a</sup>, Hyoung Jun Kim<sup>a</sup>, Suhwan Kim<sup>a</sup>, Nigel Wardell<sup>c</sup>, Riccardo Geletti<sup>c</sup>, Andrea Bergamasco<sup>f</sup>, Robert McKay<sup>g</sup>, Young Keun Jin<sup>a</sup>, Sung-Ho Kang<sup>a</sup>

<sup>a</sup> Korea Polar Research Institute, Incheon, South Korea

<sup>b</sup> University of Science and Technology-Korea, Daejeon, South Korea

<sup>c</sup> Istituto Nazionale di Oceanografia e di Geofisica Sperimentale-OGS, Trieste, Italy

<sup>d</sup> University of Trieste, Trieste, Italy

<sup>e</sup> Research Institute of Oceanography, Seoul National University, Seoul, South Korea

<sup>f</sup> Institute of Marine Sciences-National Research Council (ISMAR-CNR), Venice, Italy

<sup>g</sup> Victoria University of Wellington, Wellington, New Zealand

### ARTICLE INFO

Editor: G.J. de Lange

Keywords:

Antarctica

Ross Sea

Seismic stratigraphy

Contourites

Glacial sediments

Sedimentary process

### ABSTRACT

Sedimentation processes influenced by late Cenozoic ice-sheet dynamics and bottom-current activity can be extracted from the seismic stratigraphic record of the Ross Sea continental slope and rise, where more continuous sedimentary successions are preserved compared to the continental shelf. In this study, we present a seismic stratigraphic analysis of the Central Basin that lies in the northwestern Ross Sea, using newly acquired and existing legacy seismic reflection data that are correlated to adjacent scientific drill sites. The chronostratigraphy of Ross Sea seismic sequences lying above the mid-Miocene sequence boundary (RSU4, ca. 16.5–15.5 Ma) is based on the former Antarctic Offshore Stratigraphy (ANTOSTRAT) project. Depth-contour and isopach maps of sedimentary sequences bounded by two major unconformities of RSU4 and RSU2 (the late Pliocene boundary, ca. 4.0–2.8 Ma) and the present-day seafloor were produced to illustrate the evolution of paleo-seafloor morphology, distribution of sediments and depocenter migration in the western Ross Sea outer margin.

The results of seismic stratigraphic analysis indicate that gravity sedimentation processes dominated the Central Basin infill up to the mid-Miocene, and then downslope sediment supply gradually diminished through the late Miocene and Quaternary, likely reflecting a shift toward a cooler, less erosive glacial regime change. Since the late Pliocene, a topset-truncated glacial prograding wedge developed in the upper continental slope at the mouth of the Joides Basin and the sediment depocenter was shifted from the basin floor to the upper slope, suggesting the more persistent occurrence of grounded ice sheets on the outer continental shelf. Meanwhile, persistent along-slope bottom-current processes formed contourites on the slope and over the crests of banks surrounding the Central Basin since the mid-Miocene. In the late Pliocene, the contourites that formed off the Joides Basin mouth were overlain by glaciogenic debris flows, while the growth of contourites continued over and along the flanks of banks, farther to the north. This suggests that along-slope bottom-current processes near the Joides Basin mouth were diminished or dominated by the glacial discharge to the continental shelf edge. The sediment stacking patterns differ between the Joides/Central Basins and the Drygalski/Adare Basins located on the westernmost Ross Sea margin, suggesting that distinctive glacial/interglacial behavior of the former grounded ice streams and sediment supplies in the troughs feeding these basins were largely controlled by the paleo-seafloor morphology of the western Ross Sea continental shelf.

\* Corresponding author at: Korea Polar Research Institute, 26 Songdomirae-ro, Yeonsu-gu, Incheon 21990, South Korea.  
E-mail address: [jkhong@kopri.re.kr](mailto:jkhong@kopri.re.kr) (J.K. Hong).

## 1. Introduction

Sedimentary processes in high-latitude continental margins are mainly controlled by ice-sheet advances and retreats on the continental shelves and by bottom-water current activity on the continental slopes and rises during glacial and interglacial periods (Anderson et al., 1979; Wright and Anderson, 1982; Rebisco et al., 1996; Alley et al., 1997; Camerlenghi et al., 1997). Reconstructing the glaciomarine sedimentary processes from geological and geophysical analysis could provide useful insight into the dynamics of Antarctic ice sheets since the onset of glaciation at ca. 34 million years ago and into the variability of bottom-water circulation (Rebisco et al., 1996, 2006; Barker et al., 1999; Uenzelmann-Neben, 2006; Cooper et al., 2009; Uenzelmann-Neben and Gohl, 2012; McKay et al., 2016).

Since the early 1970s, numerous seismic surveys and scientific drilling projects have been provided information on the crustal structures and on the stratigraphic framework of the Ross Sea, Antarctica (e.g. Houtz and Davey, 1973; Hayes and Frakes, 1975; Cape Roberts Science Team, 2000; Naish et al., 2006; Cooper et al., 2009). The sedimentary successions above the acoustic basement were divided into eight seismic sequences, termed Ross Sea Seismic Sequences (RSS-1 to RSS-8), with bounding unconformities, termed Ross Sea Unconformities (RSU6 to RSU1), defined by the Antarctic Offshore Stratigraphy project (ANTOSTRAT, 1995). Seismic stratigraphic and sediment core analyses on the continental shelf have revealed the occurrence of repetitive and frequent grounding events of the East and West Antarctic ice sheets (EAIS and WAIS) over the Ross Sea (e.g. Alonso et al., 1992; Anderson and Bartek, 1992; De Santis et al., 1999; Bart, 2003; Bart et al., 2011; Gasson et al., 2016; Levy et al., 2016) (Fig. 1) after the Middle Miocene Climatic Optimum (MMCO) at ca. 17–14.5 Ma (Zachos et al., 2001). Studies on Pleistocene and Holocene marine geological and geophysical data, including geomorphological mapping, highlighted the footprint of a large variety of subglacial erosional and depositional processes (e.g. Bart, 2004; Mosola and Anderson, 2006; McKay et al., 2012; Anderson et al., 2014; Halberstadt et al., 2016; Yokoyama et al., 2016; Lee et al., 2017) (Fig. 1a). These studies are crucial for past Antarctic ice sheet modeling and future sea-level change (e.g. Pollard and DeConto, 2009; Golledge et al., 2014; DeConto and Pollard, 2016). In contrast to the continental shelf, there have been less seismic stratigraphic studies for the Ross Sea slope and rise (e.g. Granot et al., 2010; Lindeque et al., 2016). In general, more continuous and detailed sedimentary records are preserved with minimum hiatus in this part of the Antarctic outer continental margin, but they provide a less direct signature of ice sheet advance than the less continuous continental shelf records (e.g. Barker and Camerlenghi, 2002; Cooper and O'Brien, 2004; Escutia et al., 2011). Therefore, an analysis of overall sedimentary architecture using the integration of the inner and outer continental margin sedimentary sequences could provide a better understanding of the glaciomarine sedimentary processes in the Ross Sea, and how these may relate to ice sheet expansion and contraction on the continental shelf, as well as linking to regional and global archives of late Cenozoic global climatic and oceanographic evolution.

In this study, we aim to fill a gap between the shallow- and deep-water depositional systems by analyzing the seismic sequences above the mid-Miocene glacial unconformity (RSU4, ca. 16.5–15.5 Ma) in the Central Basin, which lies in the northwestern Ross Sea continental slope and rise, using the newly acquired multichannel seismic (MCS) data and existing legacy MCS data from the Antarctic Seismic Data Library System (SDLS, Fig. 2) (Wardell et al., 2007). Four major unconformities (RSU4, RSU3-CB, RSU2 and RSU1-CB) were traced into the Central Basin, bounding the seismic sequences RSS-5 to RSS-8 (from the oldest to the youngest) as defined by previous seismic stratigraphic interpretations (Brancolini et al., 1995; De Santis et al., 1995; Bart et al., 2000; Granot et al., 2010) (Fig. 3). Seismic facies units were identified and used to infer the sedimentary processes occurring in the Central Basin since the mid-Miocene. The Ross Sea seismic sequences and their

boundaries were mapped over the western Ross Sea outer margin and allow the evolution of paleo-seafloor and distribution of sedimentary sequences in the Central Basin region to be characterized, and the late Cenozoic local and regional ice sheet dynamics and bottom-current circulation in the western Ross Sea to be reconstructed. These results will guide the location of some alternate drill sites for the International Ocean Discovery Program (IODP) Expedition 374 in 2018 (McKay et al., 2017) to understand the WAIS evolution and oceanographic controls in the Ross Sea slopes and rises, which aims to refine the chronostratigraphic framework of the seismic sequences interpreted in this paper.

## 2. Regional setting

The Ross Sea, is one of the main glacial drainage outlets of the EAIS and WAIS (Denton et al., 1989; Shipp et al., 1999; Livingstone et al., 2012; Anderson et al., 2014; Halberstadt et al., 2016) (Fig. 1a,b) and it consists of a number of rift basins and half grabens formed through the evolution of the West Antarctic Rift System (WARS) (Cooper and Davey, 1985; Behrendt et al., 1991; Cooper et al., 1991; Davey and Brancolini, 1995). In contrast to low-latitude continental shelves, the Ross Sea shelf is characterized by water depths exceeding 500 m, and an overdeepened bathymetry resulting from isostatic depression and subglacial erosion by repeated advances and retreats of grounded EAIS and WAIS (Brancolini et al., 1995; De Santis et al., 1999). The Joides and Drygalski Basins, two cross-shelf glacial troughs in the western Ross Sea, occupy major tectonic depressions bounded by high-relief banks. The Joides Basin is inferred to have been one of the main drainage pathways of EAIS-sourced ice feeding into the Ross Sea during the Last Glacial Maximum (LGM) (Anderson et al., 1992, 2014; Shipp et al., 1999; Livingstone et al., 2012; Harris et al., 2014; Halberstadt et al., 2016). The Central Basin is located seaward of the Joides Basin and, unique to the other sectors of the Ross Sea and the Antarctic margin, is a semi-closed tectonic depression surrounded by high-relief banks. The Central Basin is thought to have widened to ca. 130 km between west of the Iselin Bank and the Hallett Ridge during the process of the WARS opening, at ca. 60 Ma (Cande et al., 2000; Cande and Stock, 2004; Wilson and Luyendyk, 2009). However, due to a limited number of cross-basin geophysical data such as deep seismic, magnetic and gravity survey data in the vicinity of the Central Basin, the nature and opening history of this rifting basin remains unknown (Wilson and Luyendyk, 2009).

The Central Basin is characterized by four different morphological sectors, each presenting a unique stratigraphic evolution: (1) the Joides Basin mouth and continental slope, (2) a ponded basin in the southeastern upper slope, (3) the Central Basin floor, and (4) surrounding topographic highs such as the southern (Bank A) and northern (Bank B) basement highs, the Hallett Ridge, and the Iselin Bank (Fig. 2). The southwestern continental slope to the north of the Joides Basin mouth (Fig. 2) has a gentle gradient (ca. 1°) from 600 to 1800 m water depth. In contrast, the southeastern continental slope has an initial ca. 2° dip, from 400 to 600 m, and then it becomes steeper (ca. 4.1–6.7°) from 1000 to 1600 m. At the change of dip, it is characterized by a small intraslope basin at a depth of about 600–1000 m below the shelf edge, with a circular shape and ca. 40 km wide. The small basin is confined to the north by a tectonic basement high, Bank A (Fig. 2). We name this small intraslope basin “ponded basin” in analogy to previously described similar features (e.g. Prather, 2003; Close, 2010). The floor of the Central Basin is up to 150 km wide and 2000 m and it is flanked to the east by the Iselin Bank and to the west by the Hallett Ridge with ca. 4.2–4.6° slope gradients. It is bounded to the north by Bank B and the Scott Canyon.

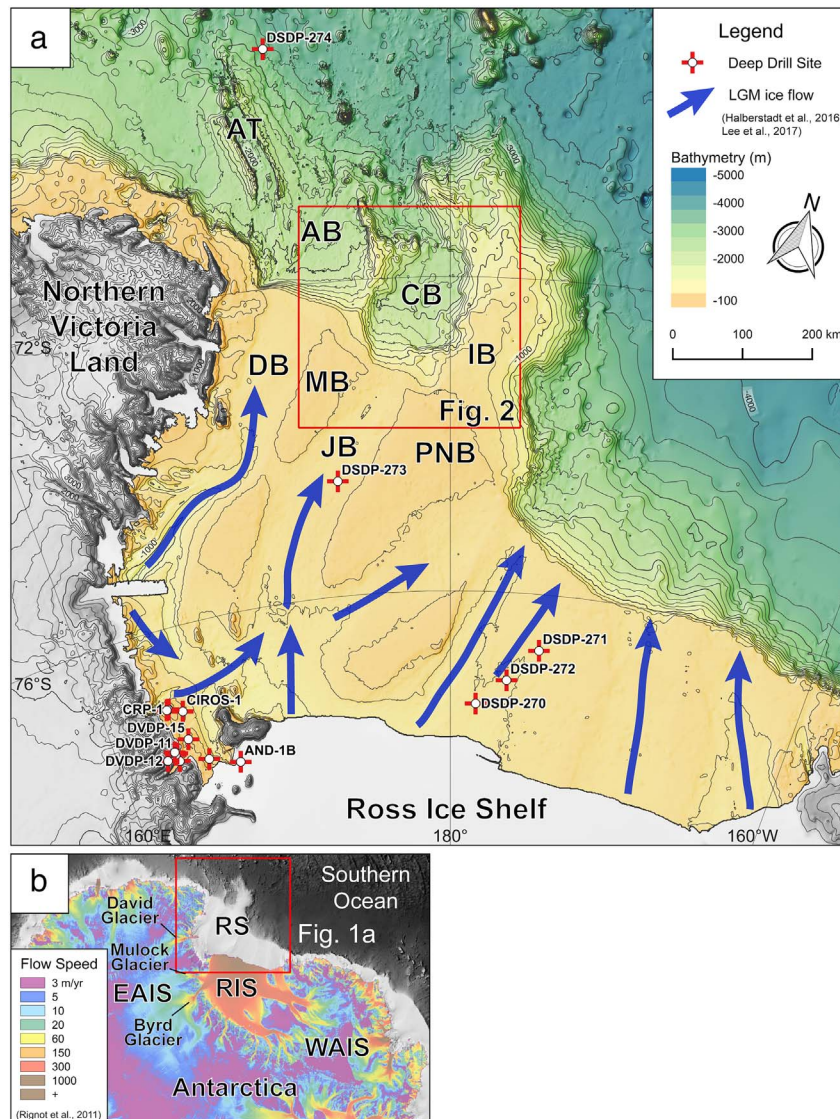


**Fig. 1.** (a) Bathymetric map of the Ross Sea (Arndt et al., 2013). The likely LGM ice flows along the main glacial troughs on the continental shelf (Halberstadt et al., 2016; Lee et al., 2017) are plotted as blue arrows. Red crosses indicate scientific drill sites in the Ross Sea shelf and rise. The red rectangle is the study area which lies on the northwestern Ross Sea slope and rise (Fig. 2). AB = Adare Basin; AT = Adare Trough; CB = Central Basin; DB = Drygalski Basin; IB = Iselin Bank; JB = Joides Basin; MB = Mawson Bank; PNB = Pennell Bank. (b) Antarctic ice sheets flow speed map of the Pacific sector of Antarctica (Rignot et al., 2011). Red rectangle indicates the Ross Sea region (Fig. 1a). EAIS = East Antarctic Ice Sheet; RIS = Ross Ice Shelf; RS = Ross Sea; WAIS = West Antarctic Ice Sheet. (For interpretation of the references to color in this figure legend, the reader is referred to the web version of this article.)

### 3. Materials and methods

#### 3.1. Data acquisition and processing

Nearly 900 km of 2D MCS data, KSL12 and KSL14, were acquired by the joint Antarctic research project of Korea (K-PORT/WARS-AMOR) and Italy (PNRA-ROSSLOPE) in the Central Basin during the IBRV Araon expeditions of in 2013 and 2015 (Fig. 2). The MCS data were recorded using a 1.5-km-long solid-type streamer with 120 channels. A seismic source consists of eight airguns and the total source volume decreased from 19.7 to 6.6 l during the data collection due to airgun problems with harsh weather conditions. The streamer and airgun array were towed at 6 m water-depth. Shot interval was 50 m and working pressure was ca. 150 bar. Shot recording time and sampling rate were 10 s and 1 ms, respectively. The fold of coverage was 1500% with a 6.25 m common mid-point (CMP) interval (Table 1).

The KSL12 and KSL14 data were processed through conventional seismic data processing steps using the GEDCO VISTA 10.0 software (Table 2). The vertical resolution of the KSL12 and KSL14 seismic data is ca. 30 m and the penetration is up to 1.8 km (ca. 2 s) below the seafloor when we assume an average-sedimentary velocity of 1850 m/s and a peak frequency of ca. 60 Hz. In order to extend the previous seismostratigraphic interpretation (e.g. ANTOSTRAT, 1995), the

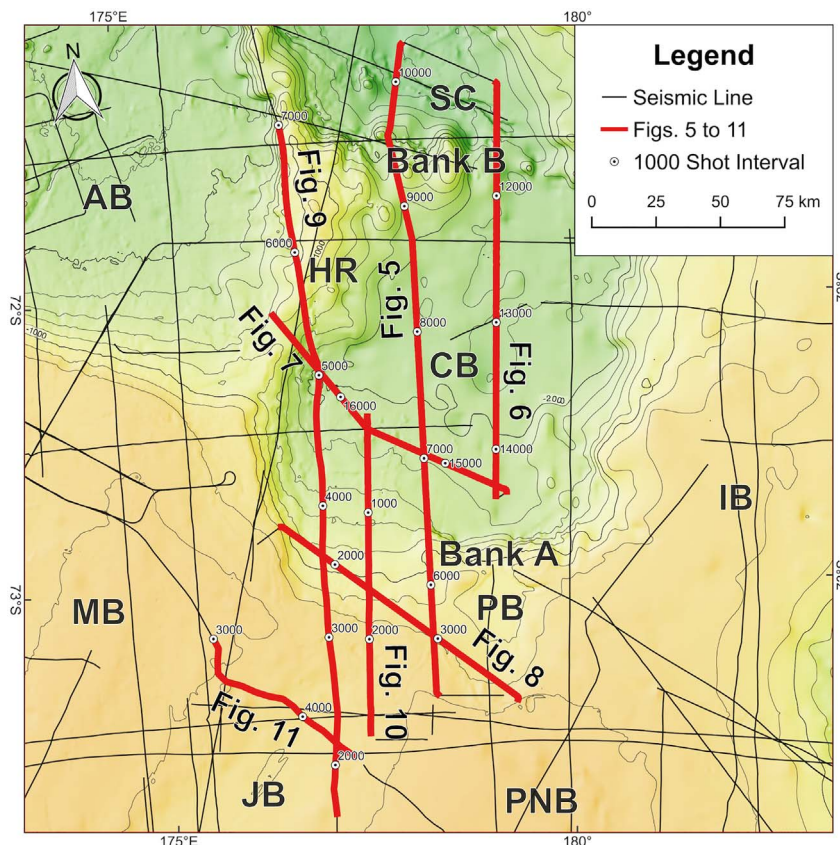
processed KSL12 and KSL14 data were integrated with existing seismic data acquired in the western Ross Sea available from the SDLS in the seismic interpretation software, SeisWare and IHS Kingdom.

#### 3.2. Seismic stratigraphic framework

We focus our study on the sedimentary successions younger than the mid-Miocene (above RSU4) due to lack of shelf-slope correlation on the seismic profiles for older sequences. It was divided into four seismic sequences, RSS-5 to RSS-8, with their bounding unconformities, RSU4 to RSU1-CB (Fig. 3a).

The former results of shelf-slope correlation in the Ross Sea margin suggested that RSU4, the lower sequence boundary of RSS-5, was formed at ca. 16.5–15.5 Ma (Brancolini et al., 1995; Brancolini and Leitchenkov, 2009; Granot et al., 2010; Lindeque et al., 2016) considering a relative low-stand sea-level (Haq et al., 1987) and age control by recovered sediment core from DSDP Site 273 (Hayes and Frakes, 1975). Meanwhile, the inner shelf drill site result in the McMurdo Sound sector (ANDRILL) proved that RSU4 was formed at ca. 14.6–14.7 Ma or ca. 13.7–14.1 Ma (Levy et al., 2016). RSU4 can be correlated across the seismic grid from the adjacent basins to Central Basin, along the outer shelf and slope sequences (Fig. 3b,c).

The upper boundary of RSS-5 in the Central Basin is named RSU3-



CB to be distinguished from the unconformity RSU3, previously defined in the Ross Sea and inferred to be formed at ca. 10.0 Ma (Brancolini et al., 1995; Brancolini and Leitchenkov, 2009; Lindeque et al., 2016). RSU3-CB cannot be directly correlated with RSU3 in the Central Basin region due to erosion of the upper part of RSS-5. We inferred that RSU3 and RSU3-CB refer to the same event based on the similar seismic characteristics and stratigraphic position between RSU4 and RSU2. IODP Expedition 374 is targeted to provide a more robust chronostratigraphic constraint for RSU3 (primary sites) and RSU3-CB (alternate sites) and will test this hypothesis (McKay et al., 2017).

RSU2 and RSU1 were previously identified and mapped only locally on the continental shelf of the Ross Sea due to the erosion of the Plio-Pleistocene sequence boundaries (ANTOSTRAT, 1995). We traced RSU2 (ca. 4.0–2.8 Ma) from the outer continental shelf beyond the Joides Basin mouth to slope and rise of the Central Basin following the former seismic stratigraphic interpretation (Brancolini et al., 1995; Granot et al., 2010) (Fig. 3b,d). A younger age for RSU2 (ca. 2.0 Ma) is suggested by piston cores of NBP94-01 and NBP03-01A cruises in the northwestern Ross Sea outer margin (Bart et al., 2011). RSU1-CB is the top of sequence RSS-7 in the Central Basin region, at the shelf edge and in the upper slope beyond the Joides Basin. The age of RSU1-CB may be ca. 0.7 Ma, assuming that it is the same event that formed RSU1 and that was previously described in the Drygalski Basin interpretation (e.g. Brancolini et al., 1995; Granot et al., 2010).

In summary, RSU4 and RSU2 are regionally correlated, and this work widens the area into which they were previously traced and mapped (Brancolini et al., 1995). In contrast, RSU3-CB and RSU1-CB are sequence boundaries that cannot be correlated regionally with the rest of the Ross Sea due to the subglacial erosion and uneven distribution of basement highs. In this study, we follow the former stratigraphic framework based on the Ross Sea shelf-slope correlations (Brancolini et al., 1995; Brancolini and Leitchenkov, 2009; Granot et al., 2010; Lindeque et al., 2016).

**Fig. 2.** Tracklines of multichannel seismic profiles can be seen in Figs. 5 to 11 (red line) and all existing data from SDLS (black line) in the Central Basin region. White circle with black dot indicates the 1000-shot point interval. Bank A = southern basement high of Central Basin; Bank B = northern basement high of Central Basin; PB = ponded basin; HR = Hallett Ridge; SC = Scott Canyon. (For interpretation of the references to color in this figure legend, the reader is referred to the web version of this article.)

### 3.3. Seismic sequence mapping and time-to-depth conversion

The RSU4 and RSU2 horizons were picked on the seismic profiles and were plotted in 500-meter resolution grids with a minimum curvature interpolation. A time-to-depth conversion was applied to the RSU4 and RSU2 grids to produce qualitative depth-contour and isopach maps in meter scale. Quantitative estimation of paleodepth contours and isopach maps cannot be made without considering sediment compaction, isostatic rebound and tectonic subsidence. This will be addressed in future work after obtaining stratigraphic constraints and physical properties of the sedimentary successions from IODP Expedition 374.

We obtained the seismic refraction velocity information of existing sonobuoy data from the ANTOSTRAT project (Cochrane et al., 1995) and from the NBPO701 cruise in the Drygalski and Adare basins (Selvans, 2011; Selvans et al., 2014). Stacking velocity information of KSL12 and KSL14 data was used for the time-to-depth conversion in the vicinity of Central Basin due to a limited number of sonobuoy data (Fig. 3b). These velocity data were converted into the time-depth domain data that were used to calculate the average sound velocity of water and sedimentary successions above RSU4 and RSU2. The depth-contours of RSU4 and RSU2 were produced using the results of multiplying RSU4 and RSU2 grids in the time domain by average sound velocity grids. Isopach maps of RSS-5/RSS-6 and RSS-7/RSS-8 were constructed by differencing for the regional unconformities, RSU4 and RSU2, and the present-day seafloor.

## 4. Results

### 4.1. Seismic facies units

#### 4.1.1. Description

Three main seismic facies were distinguished on the KSL12 and

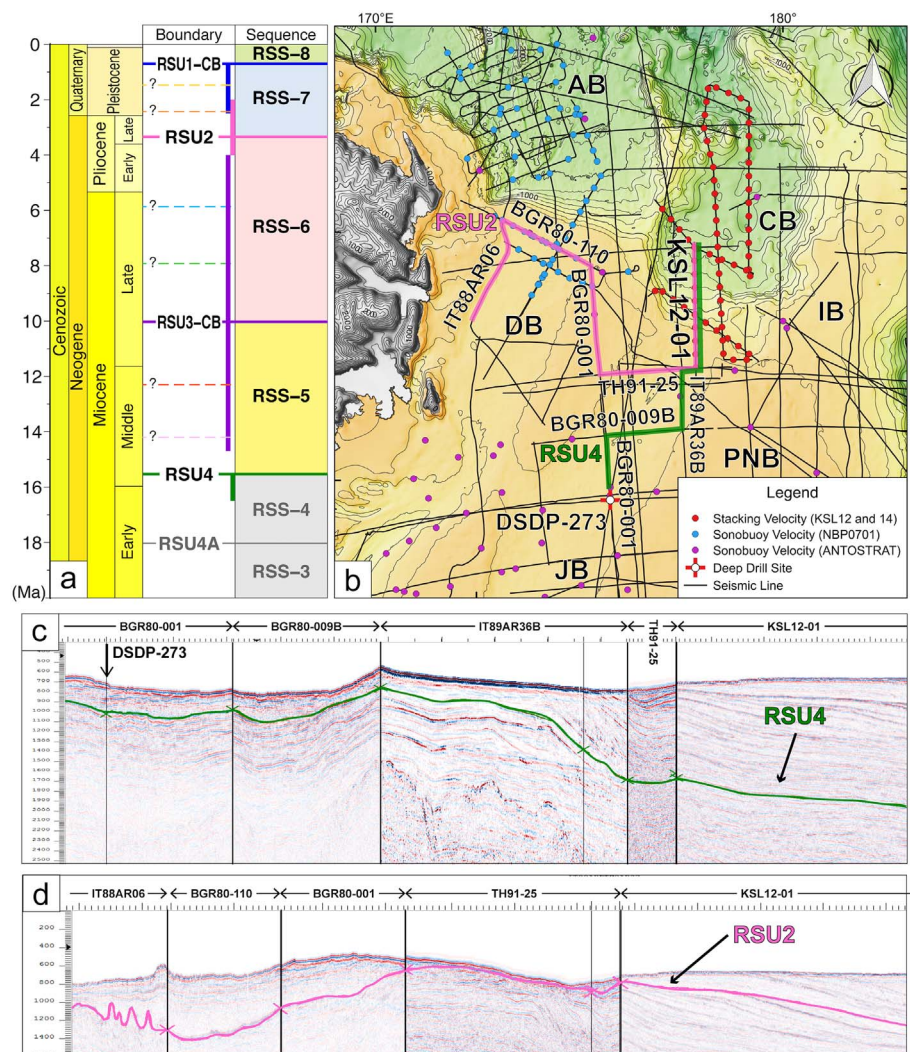


**Fig. 3.** (a) Chronostratigraphic summary for the north-western Ross Sea slope and rise for the late Cenozoic. Horizontal and vertical colored solid lines indicate major sequence boundaries and their estimated age ranges, respectively. Color dashed lines between the major sequence boundaries indicate subsequence boundaries based on the KSL12 and KSL14 profiles without age constraints. (b) Seismic correlation map of the regional unconformities, RSU4 (ca. 16.5–15.5 Ma, green line) and RSU2 (ca. 4.0–2.8 Ma, pink line), from previous studies in the western Ross Sea margin (e.g. Brancolini et al., 1995; Brancolini and Leitchenkov, 2009; Granot et al., 2010; Lindeque et al., 2016). Sonobuoy refraction velocity data for a time-to-depth conversion of the RSU4 and RSU2 grids from the NBP0701 cruise (blue dot) were used for the Drygalski Basin and Adare Basin (Selvans, 2011; Selvans et al., 2014). Additional sonobuoy data from the ANTOSTRAT project (purple dot) were used for the western Ross Sea outer margin (Cochrane et al., 1995). The stacking velocity information of KSL12 and KSL14 (red dot) was used for the Central Basin to fill the sparse sonobuoy data gap. Arbitrary seismic profiles show the correlation of (c) RSU4 and (d) RSU2 from the continental shelf to slope and rise beyond the Joides Basin and in the Central Basin according to the sedimentary records from the DSDP Leg 28 (Hayes and Frakes, 1975) and from the piston cores of NBP94-01 and NBP03-01A cruises (Bart et al., 2011). (For interpretation of the references to color in this figure legend, the reader is referred to the web version of this article.)

**Table 1**  
Acquisition parameters for the 2D multichannel seismic data, KSL12 and KSL14.

Acquisition parameter	Value
Shot interval (m)	50.0
Group interval (m)	12.5
Number of receiver group	120
Minimum offset (m)	150.0 (KSL12), 175.0 (KSL14)
Maximum offset (m)	1637.5 (KSL12), 1662.5 (KSL14)
CMP interval (m)	6.25
Fold of coverage (%)	1500
Sampling interval (ms)	1
Record length (s)	10.0

KSL14 seismic profiles in the Central Basin according to their internal configuration, lateral continuity, acoustic amplitude and frequency of internal reflections, external geometry, and location in the Central Basin (e.g. García et al., 2008; Veeken and van Moerkerken, 2013) (Fig. 4).

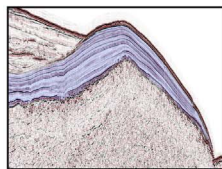
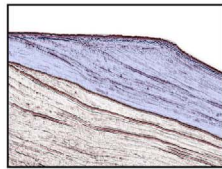
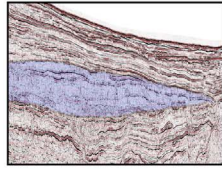
**4.1.1.1. Seismic facies unit A.** The seismic facies unit 'A' (Facies A) is characterized by subparallel, subhorizontal and/or undulated stratified reflections with high lateral continuity (> 10 km), low-to-medium amplitude and high frequency (Fig. 4). Facies A is generally observed on the crest and along the slopes of topographic highs (e.g. Banks A and B) and has a mound-shaped or sheet-like geometry.

A mound-shaped sediment body of Facies A, lying on Bank A within

**Table 2**  
Multichannel seismic data processing steps for KSL12 and KSL14.

Step	Description
A	SEG-D files input into the seismic data processing software, VISTA 10.0
B	Band-pass filtering with corner frequency of 5–8–125–250 Hz
C	Sampling rate change from 1 to 2 ms
D	Static correction for shot delay
E	Geometry setting for CMP gathering
F	Velocity analysis
G	Normal moveout correction
H	Dip moveout correction
I	CMP stack
J	Post-stack migration
K	Automatic gain control

RSS-5, thickens toward the crest (> 400 m) and pinches out basinward (SP 5700 to 6400 of KSL14-04 in Fig. 5). The southern flank of the mound-shaped deposit was partially buried by the younger RSS-6 and RSS-7, while the crest and the northern flank of the mound were still exposed at the seafloor (Fig. 5c). Facies A also occurs within sheet- and mound-shaped sediment bodies (ca. 60 km width and ca. 400 m thickness) on Bank B, within the RSS-5 to RSS-7 units (SP 8300 to 9700 of KSL14-04 in Fig. 5e), which extend eastward, over the crest of Bank B (SP 11600 to 12600 of KSL14-06 in Fig. 6). On the crest of the banks, these sedimentary deposits are thicker than the coeval sediments deposited in the Central Basin floor (Figs. 5, 6). Facies A is observed in a

Facies unit	Seismic expression	Internal configuration	Lateral continuity	Amplitude/Frequency	Geometry	Occurrence
A		Subparallel and/or undulated stratified	High	Low to medium amplitude/ High frequency	Mound- or sheet-shaped	On the crest and along the slopes of bathymetric highs
B		Subparallel and basinward dipping stratified, partly semi-transparent	Low to medium	Low to medium amplitude/ Low to medium frequency	Wedge-shaped	At the shelf edge and gentle gradient upper slope
C		Chaotic, no internal organization or poorly stratified	Low	Low to medium amplitude/ Low frequency	Lens-shaped	In the lower slope and rise of deep basin floor

**Fig. 4.** Classification of major seismic facies units in the seismic sequences based on the configuration, lateral continuity, amplitude and frequency of internal reflections and external geometry on the seismic profiles of KSL12 and KSL14 (e.g. García et al., 2008; Veeken and van Moerkerken, 2013).

mound-shaped sediment body (ca. 10 km width and up to 400 m thick) on the crest of Hallett Ridge, within RSS-6 and RSS-7 (SP 16500 to 16850 of KSL14-08 in Fig. 7), but displays a different stratal geometry above and below RSU2. The mounded deposit of RSS-6 shows internal strata that pinch out to the west and are truncated to the east by an angular unconformity, whereas the RSS-7 deposit thins toward eastern flank and thickens to the west (Fig. 7c).

Small-scale (ca. 2 km width and ca. 80 m height) undulated strata with upslope migration geometry are observed on the southern slope of the ponded basin in RSS-5, RSS-6 and in the lower part of RSS-7 (SP 3200 to 3800 of KSL14-02 in Fig. 8). This sedimentary feature can be observed on the cross seismic profiles (KSL14-03 and BGR80-001 in the lower right inset of Fig. 8b) and also on the NBP95 high-resolution single-channel seismic profiles (J.B. Anderson, Personal communication). Other undulated strata (ca. 1.5 km width and ca. 60 m height) with upslope migration and aggradation geometry developed along the eastern flank of the Hallett Ridge during the deposition of RSS-6, RSS-7 and up to present time (SP 16400 to 16500 of KSL14-08 in Fig. 7d). A compilation of multibeam bathymetry exhibits that the crests of the elongated mounds run parallel to the eastern slope of Hallett Ridge for about 5 km (lower right inset in Fig. 7b).

A large-scale (> 30 km length) undulating sedimentary sequences of RSS-5 and RSS-6 developed in front of the northern flank of Bank A (SP 6500 to 7500 of KSL14-04 in Fig. 5d). This sedimentary feature shows stratified and mounded internal configurations that is similar to Facies A, except that it shows low-to-medium lateral continuity and partly chaotic characteristics.

**4.1.1.2. Seismic facies unit B.** The seismic facies unit 'B' (Facies B) shows subparallel and basinward dipping strata with low-to-medium lateral continuity (< 10 km), low-to-medium amplitude, low-to-medium frequency, and thinning-downward wedge-shaped external geometry (Fig. 4). This facies characterizes the sequences of the continental slope at the mouth of the Joides Basin. North-south dip seismic profiles, IT89AR36B and KSL12-01, show that the wedge-shaped deposits of Facies B above RSU4 have initially sigmoidal and then tangential-oblique geometry (Figs. 9, 10).

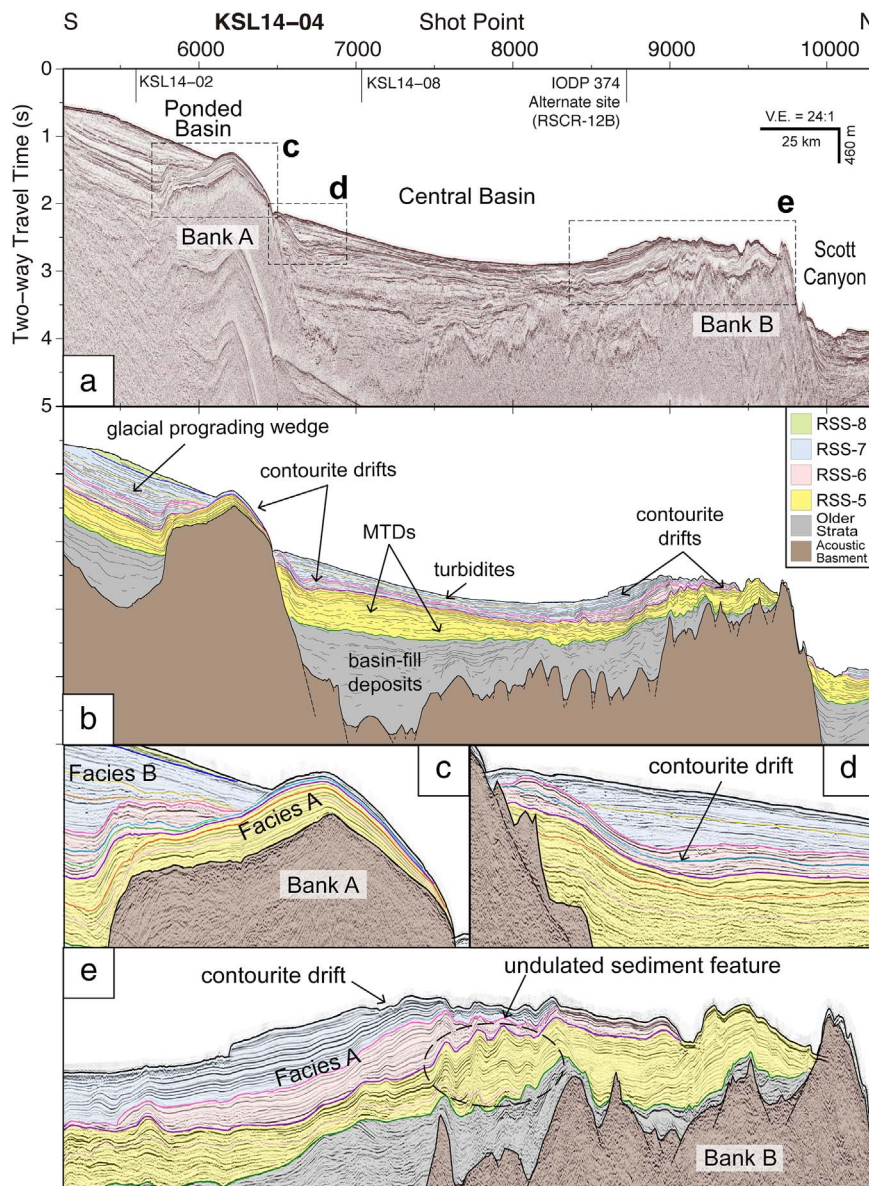
RSS-5 and RSS-6 wedge deposits show offlapping terminations of thin topset and prograding foreset beds at the paleo-shelf edge (SP 1500 to 2100 for RSS-5 and SP 2300 to 2700 for RSS-6 of IT89AR36B in

Fig. 9). RSS-5, RSS-6 and RSS-7 thin downward in the mid-lower continental slope beyond the Joides Basin (SP 700 of KSL12-01 in Fig. 10d), excluding the lower subsequence of RSS-5 that shows thickening downward. The wedge-shaped sediment body of RSS-7 (Facies B) is characterized by sharp topset truncation at the shelf edge (SP 1900 to 2600 of KSL12-01 in Fig. 10c). The chaotic and semi-transparent internal configuration of RSS-7 and RSS-8 occur near the present seafloor on the outer continental shelf of the Joides Basin (SP 1900 to 2600 of KSL12-01 in Fig. 10c). Seismic profiles parallel to the shelf edge shows that discontinuous stratified reflectors cut by erosional features in V-shape or hyperbolic point source reflections are more common in RSS-7 than in the older sequences (SP 1800 to 3400 of KSL14-02 in Fig. 8b,d). The prograding wedge of the uppermost sequence, RSS-8, lies in the outer shelf and upper slope (SP 1200 to 2200 of KSL12-01 in Fig. 10) and it does not extend into the Central Basin floor. The subparallel, stratified and higher continuity sediment layers of RSS-5, RSS-6 and RSS-7, except for the lower part of RSS-5, are observed in the lower continental slope and rise (SP 12800 to 14000 of KSL14-06 in Fig. 6; SP 15600 to 16000 of KSL14-08 in Fig. 7).

**4.1.1.3. Seismic facies unit C.** The seismic facies unit 'C' (Facies C) is characterized by chaotic internal configuration, or by strata with very low lateral continuity, low amplitude, low frequency, and lens-shaped external geometry (Fig. 4). Facies C primarily occurs on the continental slope and rise and has sharp external boundaries. The lower subsequence of RSS-5 shows downslope-thickening geometry in the lower slope beyond the Joides Basin and Central Basin floor. The lower subsequence of RSS-5 is mainly composed of large-scale (over 30 km width and 200 m thickness) lens-shaped sediment bodies (SP 6600 to 8000 of KSL14-04 in Fig. 5; SP 12800 to 26000 of KSL14-06 in Fig. 6; SP 15000 to 15800 of KSL14-08 in Fig. 7; SP 230 to 900 of KSL12-01 in Fig. 10d). In particular, a large-scale (ca. 75 km width and ca. 450 m height) convex-upward sediment body is developed in the northern part of Central Basin floor (SP 12100 to 13600 of KSL14-06 in Fig. 6c). This body contains mainly stratified and partly undulating reflections with medium lateral continuity and chaotic internal configurations.

#### 4.1.2. Interpretation

**4.1.2.1. Contourites.** Laterally continuous internal reflections suggest uniform sedimentation conditions over a large area. Low-amplitude



**Fig. 5.** (a) North-south dip seismic profile KSL14-04, crossing from the outer shelf beyond the Joides Basin through the Central Basin to Scott Canyon. (b) Line drawing of the profile shows basin-fill MTDs with Facies C and contourite drifts with Facies A on the bounding basement highs, Bank A and Bank B. Sedimentary sequences above the acoustic basement were identified with different colors following the chronostratigraphic chart in Fig. 3a. (c) Partially buried contourite drifts on the crest of Bank A. (d) Mound-shaped contourite drifts of RSS-5 and RSS-6 were buried by gravity flow deposits of RSS-7 in the northern flank of Bank A. (e) Contourite drifts and undulated sediment features on Bank B.

reflections may indicate little lithological variations in depth and high-frequency stratification reflects thin beds (Veeken and van Moerkerken, 2013). These characteristics shown by Facies A are typical of sedimentary deposits formed under the action of persistent bottom current (e.g. Faugères et al., 1999). We interpret the large-scale (> 10 km lateral extent) mound-shaped sediment bodies of Facies A, which occurs over banks (Figs. 5c,e, 6d, 7c) as contourite drifts, and the small-scale (ca. 2 km width) undulating sediments (Figs. 7d, 8c) as sediment waves or multi-crested mounded drifts formed by bottom currents that flowed along the slope and the flanks of the banks (e.g. Stoker et al., 1998; Faugères et al., 1999; Wynn and Stow, 2002; Rebisco et al., 2014; García et al., 2016; Miramontes et al., 2016).

The large-scale (> 30 km length) undulating sedimentary sequences within RSS-5 and RSS-6 in front of the northern flank of Bank A (Fig. 5d) can also be interpreted as a contourite drift (Fig. 5d), formed over irregular seafloor morphology by along-slope bottom-current processes (e.g. Faugères et al., 1999; Rebisco et al., 2014). Moderate lateral continuity and partly chaotic seismic characteristics of this sedimentary feature indicate less uniform sedimentation and lithologies both in space and in depth than the contourite drifts deposited on the

crests of Bank A, Bank B and Hallett Ridge.

**4.1.2.2. Glacial prograding wedge.** Stratified reflection packages with low-to-medium lateral continuity, as in Facies B, could indicate heterogeneous sediment deposition and occurrence of erosional surfaces (Veeken and van Moerkerken, 2013). Low-to-medium amplitude and frequency imply similar lithologies in depth sections and relatively thick beds. The wedge-shaped sedimentary sequences of Facies B with topset beds truncated by erosional surfaces or offlap termination beyond the Joides Basin mouth (Fig. 10c) have been described in polar environments as generally formed by release of debris from the base of ice grounded at the shelf edge (e.g. Vorren and Laberg, 1997; Ó Cofaigh et al., 2003). The chaotic and semi-transparent seismic facies of RSS-7 and RSS-8 in the outer continental shelf (Fig. 10c) can be interpreted as till (e.g. Dowdeswell et al., 2004; Batchelor et al., 2013). The erosional features in the glacial prograding wedge of RSS-7 (Fig. 8d) may indicate channelized bottom currents on the slope when the grounded ice sheet stayed near the paleo-shelf edge and provided subglacial meltwater (e.g. Batchelor et al., 2013). Therefore, Facies B is interpreted as a glacial prograding wedge

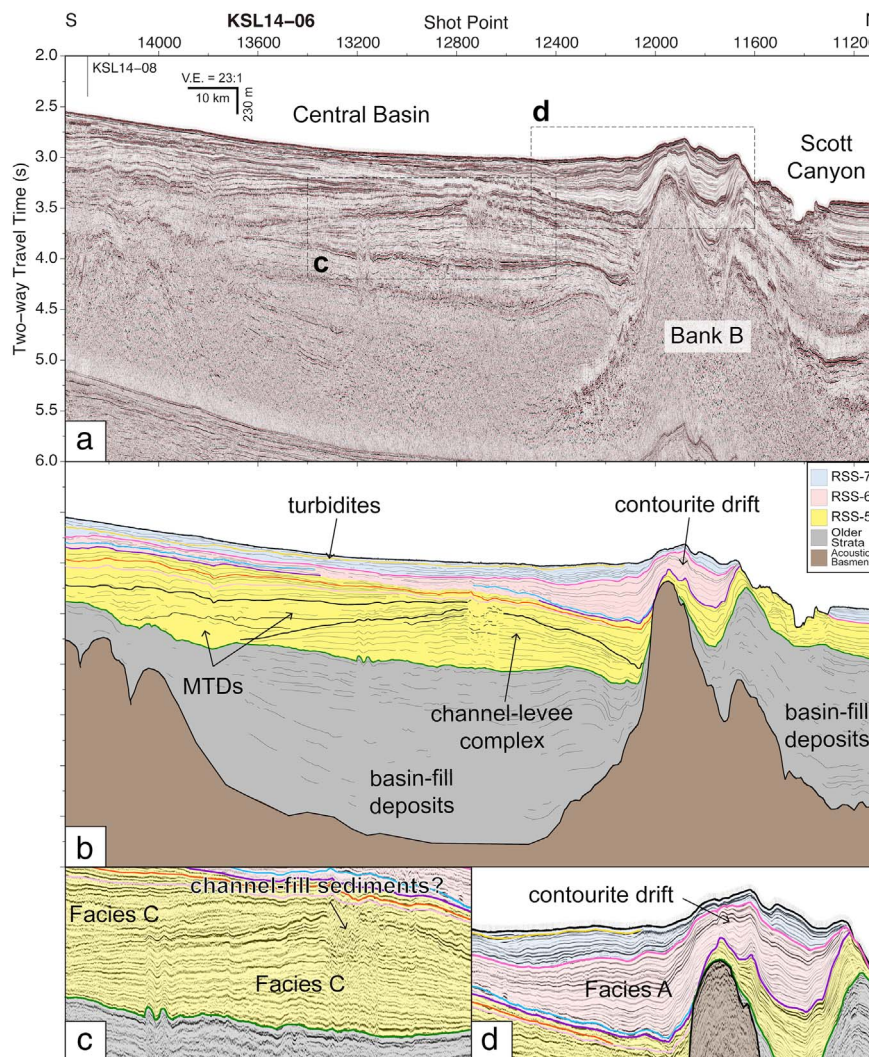


**Fig. 6.** (a) North-south seismic profile KSL14-06, crossing the northern part of the Central Basin, Bank B and Scott Canyon. (b) Line drawing of the profile shows buried channel-levee complex and MTDs on the basin floor during the early stage of RSS-5. Contourite drift with Facies A occurs on Bank B. (c) Channel-levee complex and of the lower subsequence of RSS-5 on the Central Basin floor. (d) Contourite drift with Facies A on Bank B.

composed of glaciogenic sediments transported by grounded ice sheets.

**4.1.2.3. Submarine mass transport deposits (MTDs).** The chaotic internal configuration of Facies C indicates sediments that have weak internal stratification and lens-shaped thick geometry, and are interpreted as submarine mass transport deposits (MTDs) (e.g. Arnott, 2010; Mulder, 2011; Huang and Jokat, 2016). High-amplitude, sharp lower boundaries of the lens-shaped sediment bodies indicate erosional surfaces and different physical properties between upper and lower sediment units. Units identical to Facies C are common in glacially influenced continental margins and are generally interpreted as formed by gravity-driven processes such as slumps, slides and debris flows (e.g. Donda et al., 2008; Veeken and van Moerkerken, 2013). Seismic profile IT88A-1A, which is parallel and landward of the present shelf edge, shows that the subhorizontal strata below RSU4 are cut by a channel that is filled with poorly stratified and chaotic lenses between RSU4 and present-day seafloor (Fig. 11). This combination of erosional and depositional seismic features suggest that sediments on the continental shelf were eroded and transported to the shelf edge by grounded ice sheets since RSU4 time and were redistributed to the Central Basin floor via gravity-driven slope processes. We interpret the chaotic sedimentary deposits filling the erosional channel in the outer continental shelf as a till tongue and those lying at the base of the continental slope as submarine MTDs, respectively (e.g. Collot et al., 2001; Rydningen et al., 2015; Huang and Jokat, 2016). In particular, the submarine MTDs were mainly developed during the early stage of

RSS-5 formation in the Central Basin floor (Figs. 5b, 6b, 7b, 10b).

The large-scale convex-upward sediment body in the northern part of Central Basin floor is interpret as a channel-levee complex formed during the early stage of RSS-5 formation (Fig. 6c). Its internal reflectors thin toward both sides, indicating that sediments were transported and deposited from its center to edge. The chaotic internal configuration in the center of the sediment body is indicative of erosive channel-fill sediments. Undulated reflections near the center of sediment body may be formed by over-spilling of turbidity currents (e.g. Wynn and Stow, 2002; Mulder, 2011). Similar features above RSU4 have been observed in the neighboring Adare Basin and Trough that were interpreted as a channel-levee complex formed during the same period as those in the Central Basin (Granot et al., 2010).

## 4.2. Seismic sequence maps

### 4.2.1. Time-to-depth conversion

The RSU4 depth-contour map (Fig. 12a) provides a qualitative view of paleo-seafloor morphology at the mid-Miocene in the two main glacial drainage outlets of the western Ross Sea. At RSU4 time, the paleo-shelf break of the Joides Basin was indented landward and located ca. 70 km to the south relative to the present-day shelf break, whereas the paleo-shelf break of the Drygalski Basin was located < 10 km to the south of the present shelf break (green dashed line in Fig. 12a). The RSU4 depth-contour map shows that the ponded basin is bounded by Bank A to the north and the Central Basin floor appears

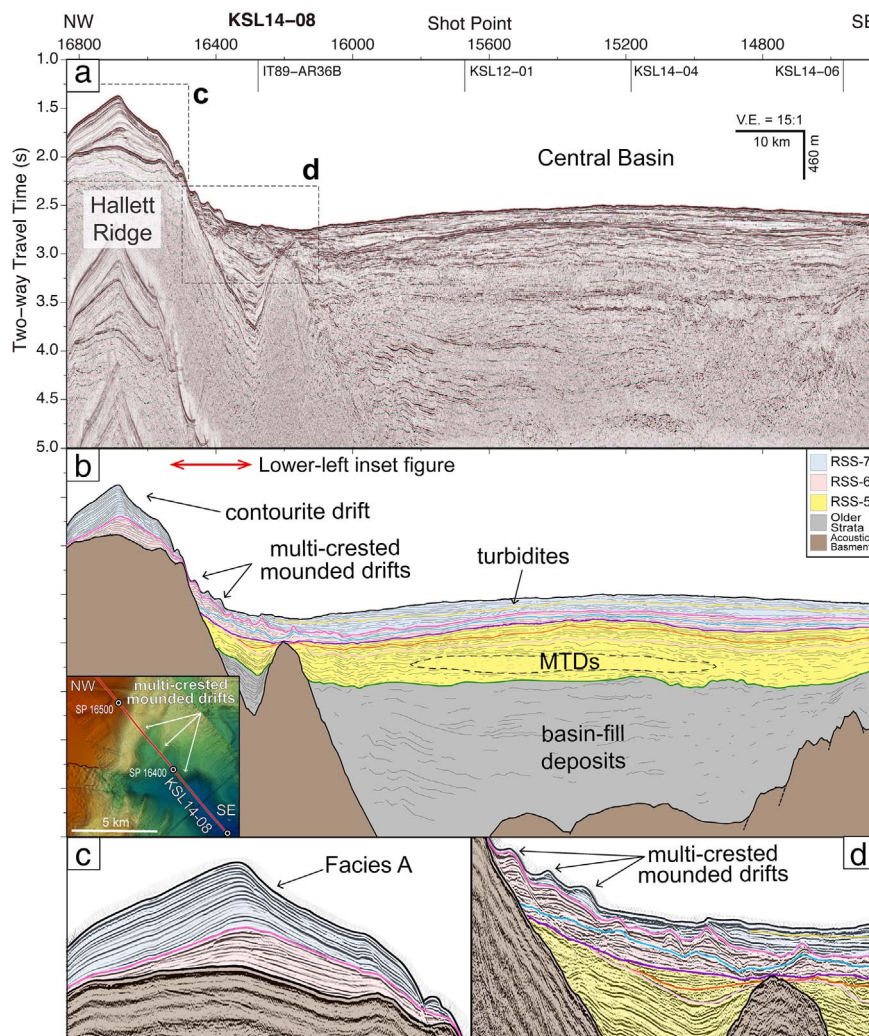


**Fig. 7.** (a) Northwest-southeast seismic profile KSL14-08, crossing the Central Basin and Hallett Ridge. (b) Line drawing of the profile shows mound-shaped contourites on the crest (Fig. 7c) and multi-crested mounded sediment drifts along the eastern flank (Fig. 7d) of Hallett Ridge. Lens-shaped MTDs and turbidites deposited the Central Basin floor. Lower left inset is a combined multibeam bathymetry image acquired during the seismic data recording (SP 16300 to 16530 of KSL14-08, red line in the inset figure) and the existing dataset (Ryan et al., 2009) shows the multi-crested mounded drifts along the eastern slope of Hallett Ridge. Blue is deep and red is shallow. White circles with black dots indicate the 100-shot point interval. (c) Mound-shaped contourite drift occurred on the crest of Hallett Ridge with Facies A. (d) The multi-crested mounded sediment drifts of RSS-6 and RSS-7 occurred along the eastern flank of Hallett Ridge. (For interpretation of the references to color in this figure legend, the reader is referred to the web version of this article.)

about a 1-km deeper than the Adare Basin floor. However, the difference in paleo-water depth between the two adjacent basins would be likely reduced after removing the sediment infill and considering the consequent isostatic adjustment.

The RSU2 depth-contour map (Fig. 12b) shows that the paleo-shelf break advanced ca. 30 km basinward at the mouth of the Joides Basin since RSU4 time (mid-Miocene to early Pliocene). However, it was nearly stationary and located near the present-day self-break at the mouth of Drygalski Basin (pink dashed line in Fig. 12b). The ponded basin and Bank A show a more gentle relief than the RSU4 surface. In addition, the elevation difference between the Central Basin floor and surrounding bathymetric highs at RSU4 time was decreased from ca. 2000 to 1000 m by RSU2 time because of sediment infill. The Central Basin floor at RSU2 time shows a flatter morphology than at RSU4 time and a similar depth of the Adare Basin floor.

#### 4.2.2. Sediment thickness

The isopach map of RSS-5 and RSS-6 (from RSU4 to RSU2 times) shows three separate depocenters in the Joides/Central Basins: (1) at the shelf edge and slope beyond the Joides Basin with a maximum sediment thickness of 1000 m, (2) in the ponded basin with a maximum sediment thickness of 600 m, and (3) in the Central Basin with a maximum sediment thickness of 800 m (Fig. 12c). Sediment packages < 200 m thick were deposited on the crests of Hallett Ridge and Bank B during this period. In contrast, most of the sediments were concentrated at the paleo-shelf break off the Drygalski Basin and sediments < 200 m thick were deposited in the Adare Basin floor.

The isopach map of RSS-7 and RSS-8 (from RSU2 time to the present) shows that a large sediment depocenter (> 400 m) formed off the paleo-shelf break of the Joides Basin, as opposed to the Drygalski Basin where the thickest sediment (> 700 m) deposit occurs on the continental shelf, behind the paleo-shelf break (Fig. 12d). Sediment deposited on the surrounding bathymetric highs of the Central Basin during this period has an average thickness of 200 m. To summarize, we observe that the overall sediment depocenter shifted landward from the Central Basin floor to the upper slope beyond the Joides Basin, whereas the sediment depocenter in the Drygalski/Adare Basins became widely distributed on the outer continental shelf.

## 5. Discussion

### 5.1. Seismic stratigraphic evidence for sedimentation processes

#### 5.1.1. Mid-late Miocene sequence (RSS-5)

RSU4, the lower sequence boundary of RSS-5, is interpreted to reflect ice expansion over the continental shelf when large volumes of sediments were eroded and transported by expanded outlet glaciers possibly sourced from the Transantarctic Mountains glaciers (e.g. the David, Mulock and Byrd Glaciers; Fig. 1b). These glaciers perhaps converged to carve the paleo-Joides Basin to the paleo-shelf edge and delivered sediments to the slope and the Central Basin floor. However, several older and younger erosional surfaces with similar geometry are observed below and above the erosional unconformity RSU4 in the same location (Fig. 11), suggesting that the paleo-Joides Basin has been

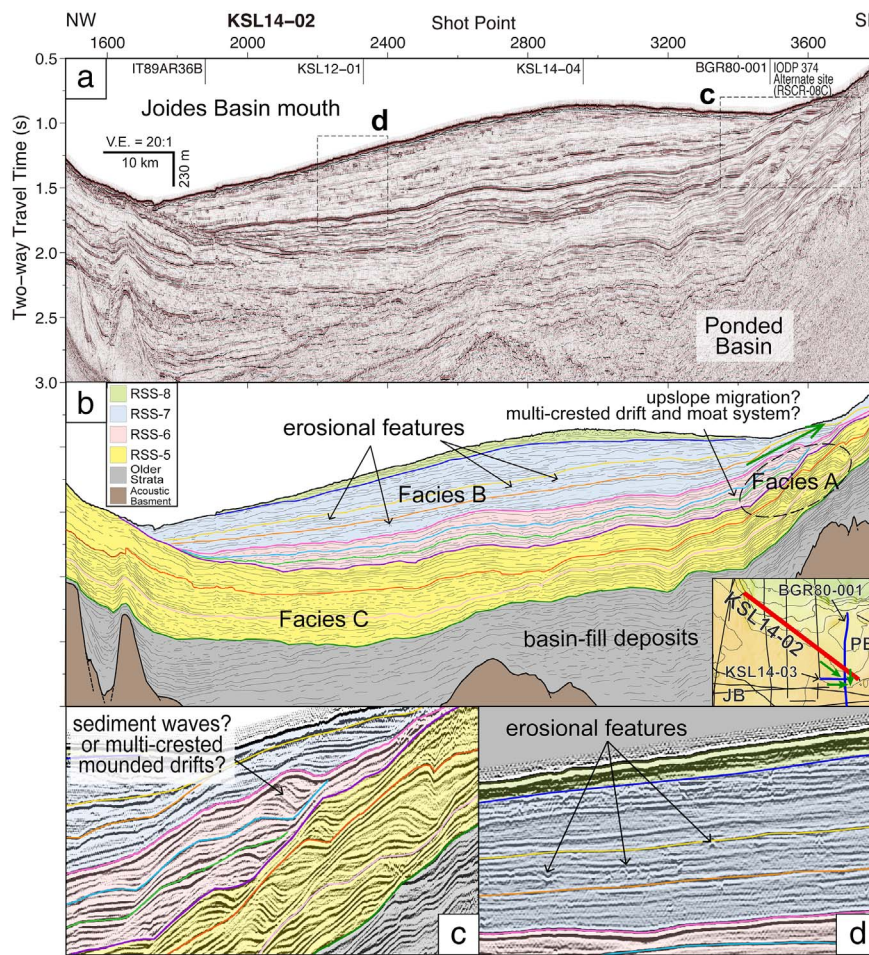


**Fig. 8.** (a) Northwest-southeast seismic profile KSL14-02, obliquely crossing the upper continental slope and ponded basin beyond the Joides Basin. (b) Line drawing of the profile shows that stacked debris flows were deposited on the upper slope, while contourites accumulated on the southern slope of ponded basin above the mid-Miocene sequence boundary. Lower right inset shows the location of the seismic profile (red line) and existing seismic lines (black lines). Blue lines in the location map indicate the intersecting seismic profiles showing sediment waves or multi-crested, mounded drifts oriented north-northeast–south-southwest. Green arrows in the line drawing and location map indicate upslope migration direction of the inferred sediment waves on three seismic profiles, KSL14-02, KSL14-03 and BGR80-001. (c) Sediment waves or multi-crested mounded drifts of RSS-5, RSS-6 and the early stage of RSS-7 with Facies A on the southern slope of ponded basin. (d) V-shape and hyperbolic erosional features in the glacial prograding wedge of RSS-7. (For interpretation of the references to color in this figure legend, the reader is referred to the web version of this article.)

a preferential route for grounded ice flow since at least the mid-Miocene. This is consistent with DSDP site 273 that documents the occurrence of ice-proximal environmental conditions in the Joides Basin during the early-mid Miocene (Hayes and Frakes, 1975; Brancolini et al., 1995).

A basinward-thickening geometry is evident in the channel-levee complex and MTDs in the lower subsequence of RSS-5 on lower slope and Central Basin floor (Figs. 5, 6, 10). We believe that this could represent a time when large volumes of sediment-laden subglacial meltwater were being discharged at the ice sheet margin during past glacial maxima. This delivery of large volumes of sediment to shelf edge would have led to slope instability and transport into the deep basin, via active gravity processes, developing submarine channel-levee systems (Arnott, 2010; Eyles and Eyles, 2010). Geomorphic and sedimentological evidence from high elevations in the Transantarctic Mountains indicate there were periods of extensive subglacial meltwater discharge emanating from the East Antarctic margin during the Middle Miocene, but the area became hyper-arid with minimal meltwater after the Middle Miocene Climate Transition (MMCT) at ca. 14.2–13.8 Ma (Lewis et al., 2007, 2008). Sedimentary facies in the AND-1B core from the inner Ross Sea shelf near McMurdo Sound suggests that sediment-laden meltwater discharge from marine based margins of the EAIS continued into the late Miocene (11–9 Ma) (McKay et al., 2009). We believe that the early stage of RSS-5 is likely older than ca. 14 Ma, when the East Antarctic Ice Sheet displayed widespread evidence of subglacial meltwater discharge at both high and low elevations. In modern glacial settings, ice sheets and glaciers with more active subglacial meltwater systems are likely to more actively eroding sediment in the glacial catchment, resulting in greatly elevated terrigenous sedimentation rates at the ice sheet margin (McKay et al., 2009).

The middle and upper subsequences of RSS-5 show that sediments mainly lie beneath the upper slope based on the seismic profiles (Figs. 5, 6, 10), while the continental rise of the Central Basin was relatively starved, indicating that sediment gravity flow processes gradually decreased during the later stage of RSS-5 formation (after ca. 14 Ma), and may be related to the still present, but decreasing, supplies of sediment-laden subglacial meltwater discharge of the EAIS marine margin during the late Miocene (McKay et al., 2009). The preservation of offlapping strata terminations among erosional and truncational surfaces, in the upper part of the RSS-5 prograding wedge would suggest that the ice sheet was not always grounding at the shelf edge in the later stage of RSS-5, or it was less capable of deeply carving the seabed (e.g. De Santis et al., 2003) (Figs. 9, 10). Therefore, we infer that some of the subglacial sediments released at or near the grounding line were not subjected to subglacial erosion during the ice maximum expansion in the later stage of RSS-5 time following the MMCT.

Based on the seismic profiles, the crests of undulating sedimentary features of RSS-5 on the southern slope of the ponded basin can be inferred to be elongated ridges running parallel to the continental slope contours. This would indicate that the sediment waves were formed under the action of persistent westward-flowing bottom currents in the Central Basin. The undulated strata (Fig. 8c) and the occurrence of different strata packages bound by disconformity surfaces may indicate that the along-slope bottom-currents shifted up- and down-slope, possibly in response to changes in the intensity of downslope bottom water currents sourced on the continental shelf. Ross Sea Bottom Water (RSBW) outflow process is occurring today at the mouth of the Joides Basin (e.g. Budillon et al., 2011). The RSBW mixes with ambient water in the upper slope of the central Basin and flows downslope and then westward, deviated by the Coriolis force. Another possible explanation

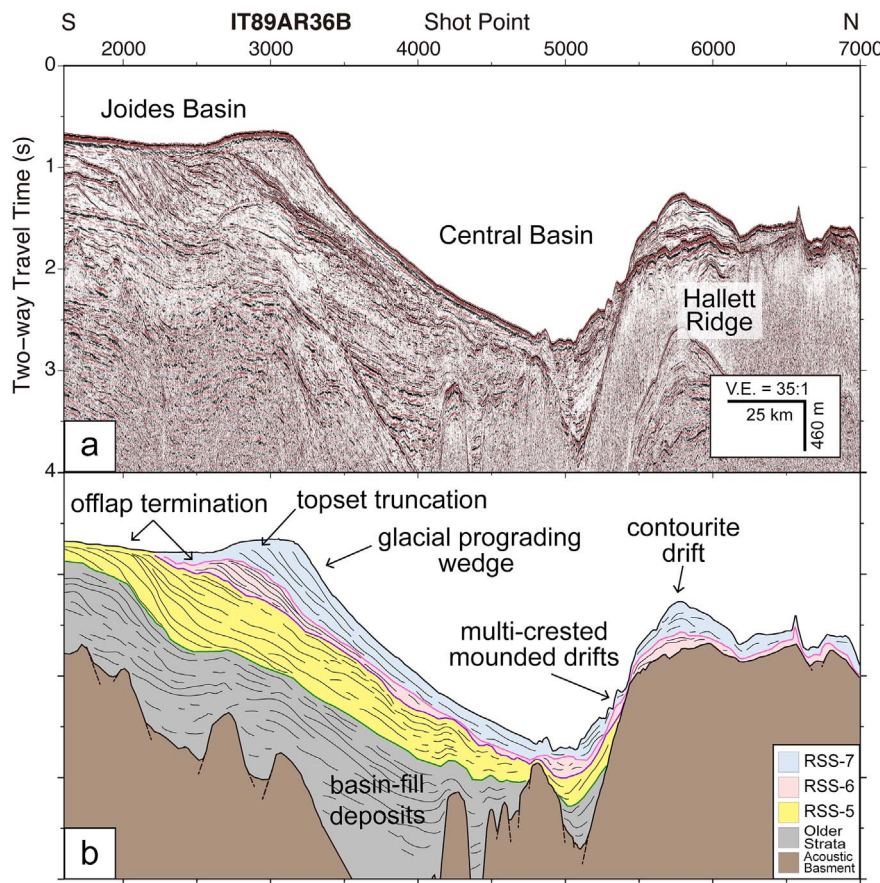


**Fig. 9.** (a) North-south, dip seismic profile IT89AR36B, crossing the Joides/Central Basins and Hallett Ridge. (b) Line drawing of the seismic profile shows the general stratal geometry and acoustic basement structure of the northwestern Ross Sea outer continental margin.

is that the westward-flowing, along-slope bottom current formed the multi-crested, mounded drifts and moat system (e.g. Stoker et al., 1998; García et al., 2016; Miramontes et al., 2016). Consequently, the crests of drifts developed parallel to slope contours.

The mound-shaped deposits on the crest of Bank A and consisting of Facies A (Fig. 5c) are interpreted as contourite drifts formed by a persistent westward-flowing bottom current. This process appears to have been established inside the ponded basin during RSS-5 formation and is consistent with the establishment or intensification of this westward current, which remains a dominant feature of Ross Sea oceanography today (e.g. Smith et al., 2012).

Sedimentary successions on Bank B are interpreted as compound of contourite drifts and sediment waves or multi-crested drifts, forming under the action of bottom currents since the formation of RSU4 (Fig. 5e) (e.g. Rebasco et al., 1996; Faugères et al., 1999; Uenzelmann-Neben, 2006; Uenzelmann-Neben and Gohl, 2012). However, it is not possible to estimate the intensity of bottom current due to lack of drill site data in the Central Basin region. We could infer that the contourites were likely sourced from settling of the fine-grained component of turbidity currents, and then entrained and transported by bottom-current over the banks surrounding the Central Basin. The peculiar seafloor morphology of the Central Basin, a semi-closed basin surrounded by banks, with an active source of sediments from the continental shelf offers a favorable setting for contourite drifts to form and to be preserved along the basin margin. In addition, the initiation of contourites at RSU4 time may coincide with the onset of the Antarctic Circumpolar Current and the clockwise rotating Ross Gyre after the complete opening of the Drake Passage in the mid-Miocene (e.g. Jacobs et al., 2002; Huang et al., 2014; Lindeque et al., 2016). The interaction of the westward-flowing southern limb of Ross Gyre and increased sediment supply to the shelf edge by expanded ice sheets was able to develop the contourite drifts along the topographic highs in the Central Basin. The

similar contourite drifts formed during the same period were observed in the continental slopes and rises of Antarctic Peninsula and Weddell Sea (e.g. Rebasco et al., 1997; Uenzelmann-Neben, 2006; Huang et al., 2014).

### 5.1.2. Late Miocene/early Pliocene sequence (RSS-6)

During the deposition of RSS-6, most of the sediments formed by gravity processes were concentrated mainly on the upper continental slope near the paleo-shelf edge and over the surrounding banks of the Central Basin (Figs. 5, 6, 7, 10). In contrast, only small amounts of sediment reached the lower continental slope and rise in the Central Basin. Turbiditic submarine channels and rare debris flows can be observed in the Central Basin, but they are much smaller than those that formed during RSS-5 deposition. RSS-6 is generally thinner than RSS-5, even though the estimated time span of RSS-6 deposition has a similar time range of ca. 5–6 million years (Fig. 3a). This basinward-thinning geometry and the reduced sedimentation rate in late Miocene is also observed in other sectors of the Ross Sea and Antarctic margin (e.g. Brancolini et al., 1995; Cooper et al., 2009). It has been interpreted as possibly related to a more polar glacial regime, that was accompanied by a reduction in turbid subglacial meltwater discharge (Brancolini et al., 1995; De Santis et al., 1995). This would imply the deposition of poorly-sorted, glaciomarine sediments in close vicinity to the ice sheet grounding line, largely through meltout of the basal debris layer. Thus, most glaciomarine sediment was sequestered in the upper continental slope where the strata consist of higher angle foreset beds than underlying strata (Barker et al., 1999; Ó Cofaigh et al., 2003; Donda et al., 2008). In more distal glaciomarine environments, the lack of turbid sediment-rich meltwater plumes would have led to reduced offshore terrigenous sedimentation. This interpretation is supported by the deposition of diatom oozes during Pliocene interglacial on the continental shelf record of AND-1B, which was interpreted as terrigenous sediment

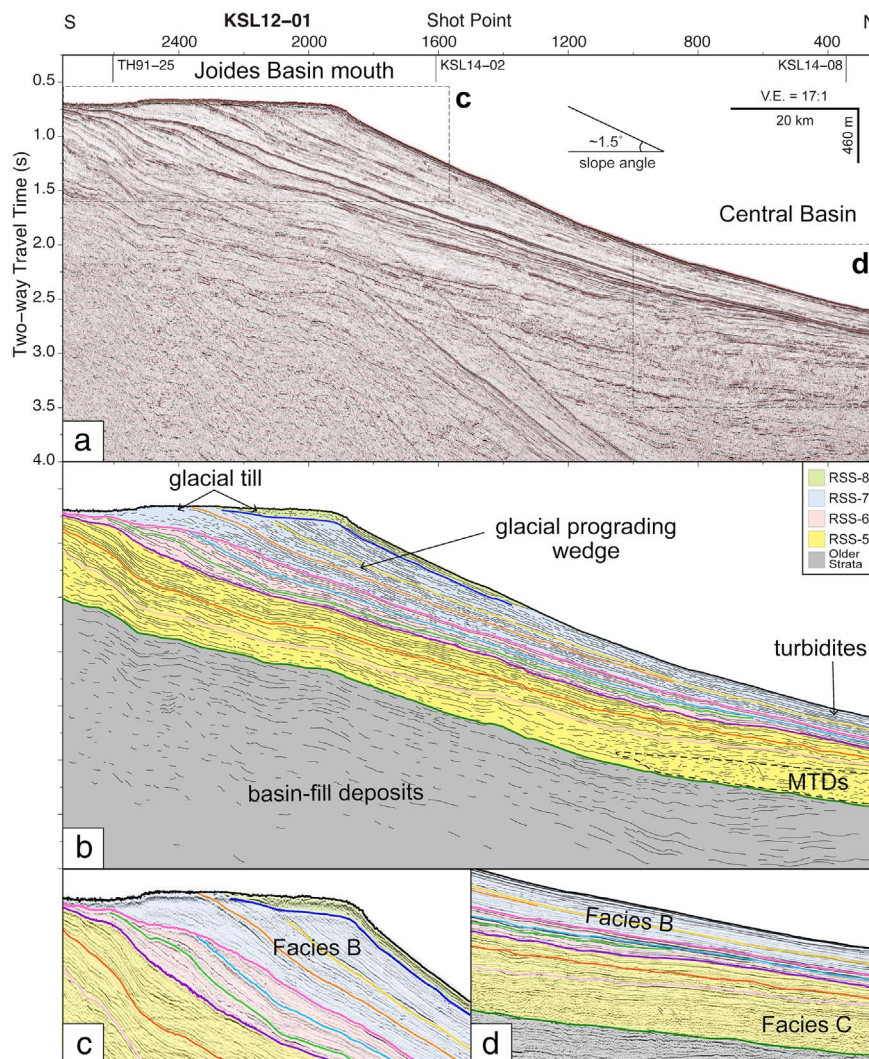


**Fig. 10.** (a) North-south dip seismic profile KSL12-01 parallel to IT89AR36B (Figs. 2, 9), through the outer continental shelf and slope beyond the Joides Basin. (b) Line drawing of the profile shows prograding paleo-shelf breaks in the outer shelf and stacked gravity flow deposits on the slope. (c) Well-developed prograding sequences with offlap termination and topset truncation. (d) MTDs with Facies C in the lower subsequence of RSS-5 and well-layered turbidites of younger sequences, RSS-6 and RSS-7 on the lower slope.

starvation during the transition toward the modern “polar” glacial regime relative to the “subpolar” glacial regime of the late Miocene (McKay et al., 2009).

In the ponded basin, the sediment waves or multi-crested mounded drifts of RSS-6 continued to develop, but the strata pinch out upslope (Fig. 8c). The mound-shaped contourite drifts that formed on the crest of Bank A during RSS-5 were partially buried by gravity flow deposits of RSS-6 (Fig. 5c). We interpret these observations as evidence of a weakening in the westward-flowing along-slope bottom current and/or diminished sediment supply from the Iselin Bank and eastern Ross Sea to the ponded basin and Bank A. The continued growth of the contourite drift of RSS-6 in front of the northern scarp of Bank A suggests that the westward-flowing bottom-currents persisted there, also during RSS-6 deposition. The drift of RSS-6 in this case is relatively thinner than the underlying drift formed during RSS-5 deposition, possibly indicating that overall sediment supply and/or bottom current energy decreased in the southern sector of the Central Basin.

During the deposition of RSS-6, elongated mounded and separated-type contourite drifts (e.g. Faugères et al., 1999; Smith et al., 2012; Rebesco et al., 2014) formed on the crest of Hallett Ridge (Fig. 7c), possibly developed under the action of westward-flowing along-slope bottom currents. These sedimentary features could indicate that along-slope sediment transportation and depositional processes were initiated prior to RSU2. Sediment sampling would be needed to understand the cause and age of this shift in sedimentation process. Shallow drilling and coring is possible since part of RSS-5, RSS-6 and RSS-7 outcrop on

the seabed over the top of Bank B and of Hallett Ridge (Fig. 5e, 7c). Piston and gravity cores have been collected recently by University of Trieste, Pusan National University and Korea Polar Research Institute (KOPRI) in the frame of the PNRA-ROSSLOPE and K-PORT projects. Although the analysis of the cores is still in progress, preliminary results show that recovered coarse sandy and mud layers could record bottom current dynamics during the last glacial and the previous interglacial cycles.

#### 5.1.3. Late Pliocene/Pleistocene sequences (RSS-7 and RSS-8)

The topset truncation of the shelf prograding foreset beds in RSS-7 suggests subglacial erosion by repeated advances and retreats of grounded ice sheet reaching the paleo-shelf break (e.g. Bart et al., 2000). The glacial prograding wedge formed at the mouth of the paleo-Joides Basin is interpreted as a trough-mouth fan (TMF) (e.g. Alonso et al., 1992; Bart et al., 2000). TMFs have been widely described from glaciated polar margins as composed of glaciogenic debris flows in the upper slope and sediment formed by suspension settling in the lower slope and rise (e.g. Vorren et al., 1989; Laberg and Vorren, 1995; Taylor et al., 2002; Ó Cofaigh et al., 2003; Huang and Jokat, 2016). Gentle upper slope gradients are favorable to stacking of glaciogenic debris flows when the grounded ice stream provides sediments beyond the shelf edge (e.g. O’Grady and Syvitski, 2002; Batchelor and Dowdeswell, 2014). Therefore, a gentle gradient (ca. 1°) of the upper slope beyond the Joides Basin was favorable to the formation of a well-developed TMF since RSU2 time. Slumps have been typically observed in the lower

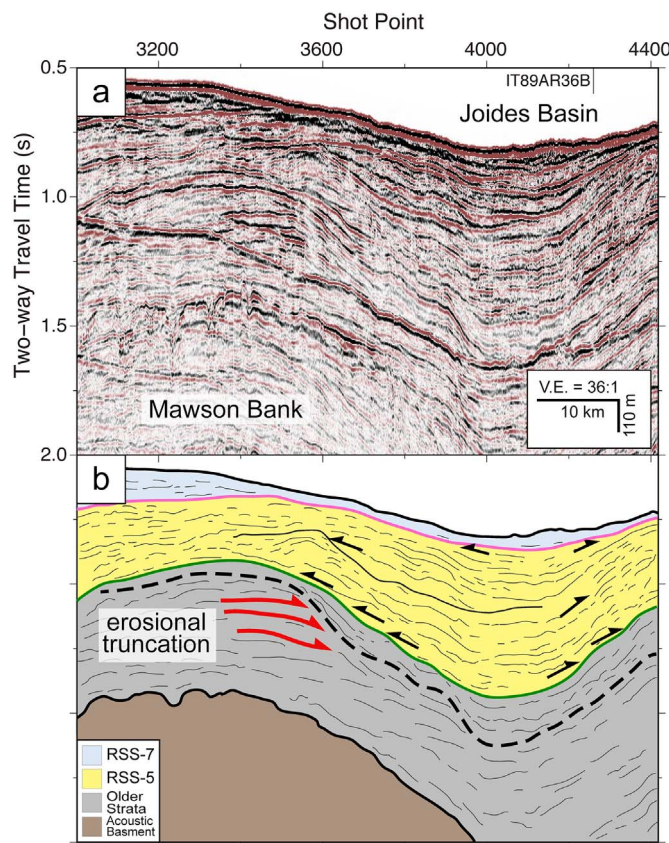


**Fig. 11.** (a) Northwest-southeast seismic profile IT88A-1A, crossing the eastern flank of Mawson Bank and Joides Basin. (b) Line drawing of the profile shows erosional truncation (red arrow) of strata below the erosional surface that formed the sea floor of the Joides Basin, at RSU4 (green line) time and earlier (older unconformity, black dashed line). (For interpretation of the references to color in this figure legend, the reader is referred to the web version of this article.)

slope of TMFs and provide sediment into the deep marine setting by generating debris and turbiditic flows, which deposit on the lower slope and rise (Ó Cofaigh et al., 2003). This could explain why RSS-7 is thicker than RSS-6 in the Central Basin floor in spite of being deposited over a shorter period (Fig. 3a).

Sediment waves or multi-crested sediment waves (Facies A) continued to form on the southern slope of the ponded basin until the early stage of the RSS-7 formation (Fig. 8c). Then gravity sedimentation processes dominated in the ponded basin and on the continental slope beyond the Joides Basin as documented by the deposition of Facies B in RSS-7 over the contourite drifts. This time corresponds to the global climate cooling after ca. 3.3 Ma and the intensified growth of sea ice in the Ross Sea that coincided with the more frequent expansion of marine-based ice sheet onto the continental shelf (McKay et al., 2012). TMF development is consistent with this interpretation, and suggests ice sheet expansion near to the shelf break occurred regularly during the late Pliocene and Pleistocene (Alonso et al., 1992). Thus, we also expect that RSBW formation increased and the westward-flowing along-slope bottom currents could have changed, as likely occurred in the adjacent Wilkes Land region (e.g. Patterson et al., 2014).

The influence of westward-flowing along-slope bottom currents on seabed deposition can still be observed along the flanks and over Bank B and Hallett Ridge in a distal setting from the shelf, during the late Pliocene to Pleistocene. The contour-parallel, elongated, multi-crested sediment drifts developed in RSS-6 and RSS-7 along the eastern flank of the Hallett Ridge (Fig. 7d) possibly formed under the action of an along-slope bottom current, deviated northward by the Hallett Ridge. The thickness change of the sediment drift over the distal Bank B, from the

mid-Miocene to the Plio-Pleistocene sequences, could reflect a weakening of the bottom-currents sediment transport and deposition capacity, possibly related to a change in the water masses salinity, temperature gradient, wind strength and suspended sediment concentration. However, stratigraphic control from shallow coring and drill sites is needed to test this hypothesis and refine the timing of these shifts in depositional settings. The thickening of sediment drift deposition from RSS-6 to RSS-7 over Hallett Ridge could be caused by an increase of sediment provided by the TMF development combined with increased along-slope current intensity.

## 5.2. Paleo-seafloor morphology and sediment thickness

On the paleo-seafloor morphology map at the time of RSU4 formation (mid-Miocene, ca. 16.5–15.5 Ma), the difference in elevation between the Central Basin floor and surrounding banks was higher than the present-day, indicating that the Central Basin was already a more closed depositional setting compared to the Adare Basin (Fig. 13a). Most sediments were delivered from the continental shelf, mainly through the paleo-Joides Basin by subglacial transportation (blue arrow in Fig. 13a), and were deposited inside the Central Basin instead of being redistributed onto the abyssal plain by turbidity currents, as was the case for the Adare Basin. Bank B may have acted as a barrier to sediment transport to the north, and therefore sediments could fill the Central Basin more readily than the Adare Basin floor. Contourites developed along the southern slope of the ponded basin, over Banks A and B, the Hallett Ridge and the Iselin Bank during the mid-Miocene to late Pliocene (red stars in Fig. 13a). These contourites are believed to have been deposited by westward-flowing, along-slope bottom currents (white arrows in Fig. 13a), constrained by the high-relief seafloor. This sedimentation process may also have occurred later than RSS-6 at the paleo-shelf edge, but we could not find any evidence of it in the seismic record because sediment gravity flows have heavily affected this area since RSU2 time (late Pliocene, ca. 4.0–2.8 Ma) (black arrows in Fig. 13b). In Plio-Pleistocene sequences, the bottom current signature can be still observed (white arrows in Fig. 13b) along the slopes and over topographic highs in a more distal setting from the outer continental shelf – e.g. on Hallett Ridge and Bank B (red stars in Fig. 13b).

The sediment thickness map shows that 600 m thick sediment depocenters are located in the Joides Basin mouth and Central Basin floor (Fig. 12c), indicating that a large amount of sediment was transported and deposited by gravity processes along the narrow and deep depressions of the former Joides Basin during the mid-late Miocene (black arrow in Fig. 13a). During the late Pliocene and Pleistocene, the sediment depocenter shifted nearer to the Joides Basin mouth (Fig. 12d), when glaciogenic debris flow deposits mainly accumulated on the continental slope (black arrow in Fig. 13b), forming the TMF. At the same time, downslope sediment transportation onto the lower slope and rise of the Central Basin diminished.

Differences between the migration of the paleo-shelf breaks of the Joides and Drygalski Basins through the late Cenozoic may be explained by different grounded ice stream flow and sediment supply, as a response to paleo-seafloor morphology and geology in the western Ross Sea continental shelf (Figs. 12, 13). According to a recent study, grounded ice streams retreated slowly from the Joides Basin and more rapidly from the Drygalski Basin after the Last Glacial Maximum (Halberstadt et al., 2016). This was possibly caused by shallower and gently overdeepened seafloor and relatively old and hard substrate in the Joides Basin relative to the Drygalski Basin (Shipp et al., 1999; Winsborrow et al., 2010; Halberstadt et al., 2016). Halberstadt et al. (2016) also suggest that the Joides Basin may have received ice from both the David Glacier to the north of Ross Island and EAIS outlets to the south of Ross Island (e.g. Byrd and Mullock Glaciers; Fig. 1a). Ice sheet modeling experiments indicate that these glaciers (esp. Byrd and David glaciers) had high ice fluxes resulting in a higher cumulative sediment flux at the past ice sheet grounding line (Golledge et al.,

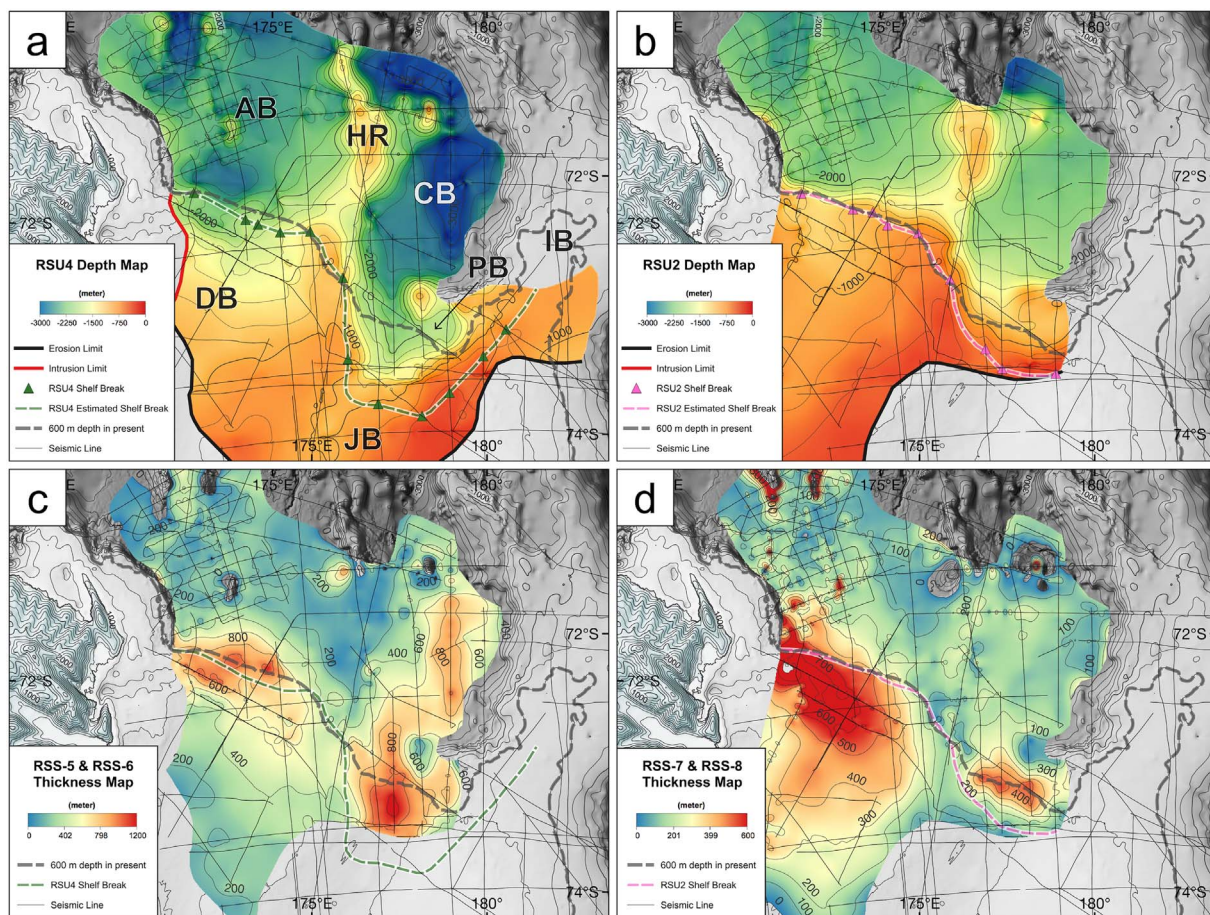


**Fig. 12.** Depth-contour maps of the (a) RSU4 and (b) RSU2 surfaces provide the general paleo-seafloor morphology at the middle Miocene (ca. 16.5–15.5 Ma) and late Pliocene-early Pleistocene (ca. 4.0–2.8 Ma), respectively. Erosion (black line) and intrusion (red line) limits of the RSU4 and RSU2 surfaces are from the ANTOSTRAT project (1995). Paleo-shelf breaks observed on the seismic profiles (green and pink triangles and dashed lines) and the present-day shelf break at 600-m isodepth contour (gray dashed line) indicate the evolution of the northwestern Ross Sea margin. Black solid lines mean multichannel seismic lines. Isopach maps of (c) RSS-5 and RSS-6 (mid-Miocene to early Pliocene, RSU4 to RSU2), and (d) RSS-7 and RSS-8 (late Pliocene to Pleistocene, RSU2 to the present seafloor) show the sediment thickness, distribution and shifting of sediment depocenters through the late Cenozoic. (For interpretation of the references to color in this figure legend, the reader is referred to the web version of this article.)

2013). Combining high ice and sediment flux with longer residence times at the shelf break during glacials would explain the larger glacial prograding wedge forming in the Joides Basin mouth. In addition, the east-west extension of the WARS in the Joides/Central Basins took place ca. 30 m.y. earlier than in the Drygalski/Adare Basins (Wilson and Luyendyk, 2009; Wilson et al., 2012). This relatively older rift system in the Joides/Central Basins could not provide a deep, wide, and actively subsiding accommodation space for proglacial sediments to accumulate on the outer shelf behind the paleo-shelf break unlike the Drygalski/Adare Basins (Fig. 12c,d).

## 6. Conclusions

Compilation of the new and existing seismic data correlated with adjacent scientific drill site data allowed us to extend the former Ross Sea seismic stratigraphic interpretation (ANTOSTRAT, 1995) of mid-Miocene to Plio-Pleistocene sequences into the Central Basin region, in the northwestern Ross Sea slope and rise. Seismic facies units were classified and sequence maps were produced to reconstruct the sedimentation processes in association with ice sheet dynamics and bottom current activity during the late Cenozoic.

The Joides Basin was carved by EAIS sourced marine-based ice sheets expanding into the Ross Sea since the mid-Miocene (RSU4, ca. 16.5–15.5 Ma), a process that has delivered a large amount of sediment to the Joides and Central Basins. The redistributed sediments formed channel-levee complexes and MTDs, which filled the Central Basin floor

during the early stage of RSS-5 formation. However, sediments within younger sequences above the lower subsequence of RSS-5 accumulated at the Joides Basin mouth, where a glacial prograding wedge developed. We interpret this as reflecting a cooling Antarctic glacial regime in the western Ross Sea, whereby during the mid-late Miocene frequent grounded ice sheet fluctuations over the shelf delivered a large volume of glaciomarine muds via turbid subglacial meltwater discharge. However, during the latest Miocene and Pliocene, subglacial meltwater discharge significantly decreased as the ice sheet evolved toward its modern polar-style glacial regime. Distal glaciomarine environments became increasingly sediment starved. This is evident in Central Basin where poorly sorted glacial sediments accumulated on the shelf edge and upper slope and only small amounts of sediment reached the deep basin floor. Since the late Pliocene (RSU2, ca. 4.0–2.8), a topset truncated TMF developed in the outer shelf and upper slope and the sediment depocenter shifted from the Central Basin floor to the upper slope. We interpret this as indicating more regular expansion of grounded marine ice sheets further basinward during the late Pliocene cooling. This acted to provide glaciogenic debris flows to the Joides Basin mouth.

The high-relief topography and the unique semi-closed setting of the Central Basin favored the development of contourites associated with westward-flowing along-slope bottom currents inside the Central Basin and ponded basin. The mid-Miocene sequence boundary (RSU4) marks the time when contourite drifts started growing in this sector of the Antarctic margin. After the time of RSU2, contourites formed along the

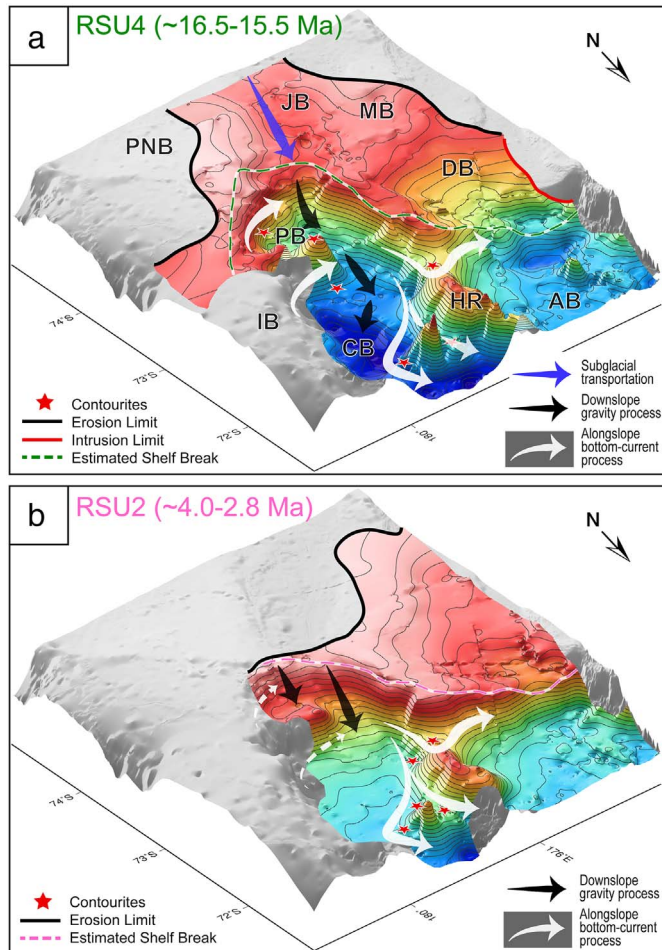


**Fig. 13.** Perspective views of paleo-seafloor morphology (100 m contours) in the Central Basin region at the times of (a) RSU4 and (b) RSU2 are shown with the inferred bottom-current (white arrows) and gravity flow (black arrows) sedimentation processes. Blue is deep and red is shallow. Grayscale indicates the present-day bathymetry out of the paleo-seafloor morphology grid limit. Blue arrow in Fig. 13a indicates subglacial sediment transportation. Dashed white arrows in Fig. 13b are weakened bottom-current process. Red stars indicate the locations of contourite sediment drifts observed on the seismic profiles. Green and pink dashed lines are the estimated paleo-shelf breaks at RSU4 and RSU2 times. Black and red lines indicate erosion and intrusion limits, respectively. (For interpretation of the references to color in this figure legend, the reader is referred to the web version of this article.)

southernmost sectors of the Central Basin and ponded basin were buried by gravity flow deposits. This was caused by the overall advance of the Joides Basin glacial drainage system basinward, which coincided with the TMF formation during the late Pliocene. During the same period, bottom currents remained active and deposited contourites in areas that were more remote from this direct glacial sediment pathway. This may indicate that the overall bottom current pathway along the Antarctic continental margin is mainly influenced by seafloor morphology and grounded ice-sheet dynamics.

The difference of depositional trends between the Joides/Central Basins and the Drygalski/Adare Basins may reflect contrasting ice stream behaviors controlled by former seafloor morphology, geology, glacial rheology and sediment fluxes related to ice sheet dynamics. Relatively dynamic ice streams with a high ice and sediment flux in the Joides Basin extended farther basinward and built a prograding stratal geometry at the paleo-shelf break. However, the ice stream in Drygalski Basin concentrated most of the sediments on the outer shelf behind the paleo-shelf break with lower ice flow and less sediment supply than the Joides Basin.

## Acknowledgement

The authors are grateful to the support of the captain and crew of the RVIB Araon during the Antarctic expeditions of ANA03B and ANA05B. We acknowledge that the Seismic Data Library System (SDLS) allows free access to all existing MCS data in the study area. We thank J.B. Anderson for providing the high-resolution seismic data of NBP95 in the western Ross Sea margin. This work was supported by the Korea Polar Research Institute Grants (PM15040 and PE17050) and the ROSSLOPE project (PdR 2010/A.2.07 and PdR 2013/AN2.01) of the Italian Antarctic Research Program (PNRA). We used the SeisWare (KOPRI-UST) and IHS Kingdom (OGS) for seismic correlation, sequence mapping and depth conversion under the university grant programs. Many thanks to Gert J. de Lange, Philip O'Brien and an anonymous reviewer for providing many helpful comments and suggestions for improving the manuscript.

## References

- Alley, R., Cuffey, K., Evenson, E., Strasser, J., Lawson, D., Larson, G., 1997. How glaciers entrain and transport basal sediment: physical constraints. *Quat. Sci. Rev.* 16, 1017–1038.
- Alonso, B., Anderson, J.B., Díaz, J.I., Bartek, L.R., 1992. Pliocene-Pleistocene seismic stratigraphy of the Ross Sea evidence for multiple ice sheet grounding episodes. In: Elliot, D.H. (Ed.), *Contributions to Antarctic Research III*, Antarctic Research Series. vol. 57. American Geophysical Union, Washington D.C., pp. 93–103.
- Anderson, J.B., Bartek, L.R., 1992. Cenozoic glacial history of the Ross Sea revealed by intermediate resolution seismic reflection data combined with drill site information. In: Kennett, J.P., Warkne, D.A. (Eds.), *The Antarctic Paleoenvironment: A Perspective on Global Change: Part One*, Antarctic Research Series. vol. 56. American Geophysical Union, Washington D.C., pp. 231–263.
- Anderson, J.B., Kurtz, D., Weaver, F.M., 1979. Sedimentation on the Antarctic continental slope. In: Doyle, L.J., Pilkey, O. (Eds.), *Geology of Continental Slopes*, Special Publication SEPM, Tulsa, pp. 265–283.
- Anderson, J.B., Shipp, S.S., Bartek, L.R., Reid, D.E., 1992. Evidence for a grounded ice sheet on the Ross Sea continental shelf during the late Pleistocene and preliminary paleodrainage reconstruction. In: Elliot, D.H. (Ed.), *Contributions to Antarctic Research III*, Antarctic Research Series. American Geophysical Union, Washington D.C., pp. 39–62.
- Anderson, J.B., Conway, H., Bart, P.J., Witius, A.E., Greenwood, S.L., McKay, R.M., Hall, B.L., Ackert, R.P., Licht, K., Jakobsson, M., Stone, J.O., 2014. Ross Sea paleo-ice sheet drainage and deglacial history during and since the LGM. *Quat. Sci. Rev.* 100, 31–54.
- ANTOSTRAT, 1995. Seismic stratigraphic atlas of the Ross Sea, Antarctica. In: Cooper, A.K., Barker, P.F., Brancolini, G. (Eds.), *Geology and Seismic Stratigraphy of the Antarctic Margin*, Antarctic Research Series. American Geophysical Union, Washington D.C.
- Arndt, J.E., Schenke, H.W., Jakobsson, M., Nitsche, F.O., Buys, G., Goleby, B., Rebasco, M., Bohoyo, F., Hong, J., Black, J., Greku, R., Uditsev, G., Barrios, F., Reynoso-Peralta, Walter, Taisei, Morishita, Wigley, Rochelle, 2013. The International Bathymetric Chart of the Southern Ocean (IBCSO) version 1.0—a new bathymetric compilation covering circum-Antarctic waters. *Geophys. Res. Lett.* 40, 3111–3117.
- Arnott, R.W.C., 2010. Deep-marine sediments and sedimentary systems. In: James, N.P., Dalrymple, R.W. (Eds.), *Facies Models 4*, GEOText. The Geological Association of Canada, pp. 295–322.
- Barker, P.F., Camerlenghi, A., 2002. Glacial history of the Antarctic Peninsula from Pacific margin sediments. *Proc. Ocean Drill. Program Sci. Results* 178, 1–40.
- Barker, P.F., Barrett, P.J., Cooper, A.K., Huybrechts, P., 1999. Antarctic glacial history from numerical models and continental margin sediments. *Palaeogeogr. Palaeoclimatol. Palaeoecol.* 150, 247–267.
- Bart, P.J., 2003. Were West Antarctic ice sheet grounding events in the Ross Sea a consequence of East Antarctic ice sheet expansion during the middle Miocene? *Earth Planet. Sci. Lett.* 216, 93–107.
- Bart, P.J., 2004. West-directed flow of the West Antarctic ice sheet across eastern basin, Ross Sea during the quaternary. *Earth Planet. Sci. Lett.* 228, 425–438.
- Bart, P., Anderson, J., Trincardi, F., Shipp, S., 2000. Seismic data from the Northern basin, Ross Sea, record extreme expansions of the East Antarctic Ice Sheet during the late Neogene. *Mar. Geol.* 166, 31–50.
- Bart, P.J., Sjumneskog, C., Chow, J.M., 2011. Piston-core based biostratigraphic constraints on Pleistocene oscillations of the West Antarctic Ice Sheet in western Ross Sea between North Basin and AND-1B drill site. *Mar. Geol.* 289, 86–99.
- Batchelor, C.L., Dowdeswell, J.A., 2014. The physiography of High Arctic cross-shelf troughs. *Quat. Sci. Rev.* 92, 68–96.
- Batchelor, C.L., Dowdeswell, J.A., Pietras, J.T., 2013. Seismic stratigraphy, sedimentary architecture and palaeo-glaciology of the Mackenzie Trough: evidence for two Quaternary ice advances and limited fan development on the western Canadian Beaufort Sea margin. *Quat. Sci. Rev.* 65, 73–87.
- Behrendt, J., LeMasurier, W., Cooper, A., Tessensohn, F., Trehe, A., Damaske, D., 1991. Geophysical studies of the West Antarctic rift system. *Tectonics* 10, 1257–1273.
- Brancolini, G., Leitchenkov, G., Cooper, et al., 2009. Cenozoic climate history from seismic reflection and drilling studies on the Antarctic Continental margin. In:

- Florindo, F., Siegert, M.J. (Eds.), Antarctic Climate Evolution. Developments in Earth and Environmental Sciences Elsevier, pp. 118–126.
- Brancolini, G., Cooper, A.K., Coren, F., 1995. Seismic facies and glacial history in the western Ross Sea (Antarctica). In: Cooper, A.K., Barker, P.F., Brancolini, G. (Eds.), Geology and Seismic Stratigraphy of the Antarctic Margin. Antarctic Research Series Wiley Online Library, pp. 209–233.
- Budillon, G., Castagno, P., Aliani, S., Spezie, G., Padman, L., 2011. Thermohaline variability and Antarctic bottom water formation at the Ross Sea shelf break. *Deep Sea Res. Part Oceanogr. Res. Pap.* 58, 1002–1018.
- Camerlenghi, A., Crise, A., Pudsey, C., Acerboni, E., Laterza, R., Rebesco, M., 1997. Ten-month observation of the bottom current regime across a sediment drift of the Pacific margin of the Antarctic Peninsula. *Antarct. Sci.* 9, 426–433.
- Cande, S.C., Stock, J.M., 2004. Constraints on Late Cretaceous and Cenozoic extension in the Ross Sea from the southwest Pacific plate circuit. *EOS Trans. Am. Geophys. Union* 85.
- Cande, S.C., Stock, J.M., Müller, R.D., Ishihara, T., 2000. Cenozoic motion between east and west Antarctica. *Nature* 404, 145–150.
- Cape Roberts Science Team, 2000. Studies from the Cape Roberts project, Ross Sea, Antarctica. Initial report on CRP-3. *Terra Antarct.* 7 (1/2), 1–209.
- Close, D., 2010. Slope and fan deposition in deep-water turbidite systems, East Antarctica. *Mar. Geol.* 274, 21–31.
- Cochrane, G.R., De Santis, L., Cooper, A.K., 1995. Seismic velocity expression of Glacial sedimentary rocks beneath the Ross Sea from sonobuoy seismic-refraction data. In: Cooper, A.K., Barker, P.F., Brancolini, G. (Eds.), Geology and Seismic Stratigraphy of the Antarctic Margin. Antarctic Research Series Wiley Online Library, pp. 261–270.
- Collot, J., Lewis, K., Lamarche, G., Lallemand, S., 2001. The giant Ruatoria debris avalanche on the northern Hikurangi margin, New Zealand: result of oblique seamount subduction. *J. Geophys. Res. Solid Earth* 106, 19271–19297.
- Cooper, A.K., Davey, F.J., 1985. Episodic rifting of Phanerozoic rocks in the Victoria Land Basin, western Ross Sea, Antarctica. *Science* 229, 1085–1087.
- Cooper, A.K., O'Brien, P.E., 2004. Leg 188 synthesis: transitions in the glacial history of the Prydz Bay region, East Antarctica, from ODP drilling. In: Cooper, A.K., O'Brien, P.E., Richter, C. (Eds.), Proceedings of the Ocean Drilling Program, Scientific Results. Ocean Drilling Program, pp. 1–42.
- Cooper, A.K., Davey, F.J., Hinze, K., 1991. Crustal extension and origin of sedimentary basins beneath the Ross Sea and Ross Ice Shelf, Antarctica. In: Thomson, M.R.A., Crame, J.A., Thomson, J.W. (Eds.), The Geological Evolution of Antarctica. Cambridge University Press, pp. 285–291.
- Cooper, A.K., Brancolini, G., Escutia, C., Kristoffersen, Y., Larter, R., Leitchenkov, G., O'Brien, P., Jokat, W., 2009. Cenozoic climate history from seismic reflection and drilling studies on the Antarctic continental margin. In: Florindo, F., Siegert, M. (Eds.), Antarctic Climate Evolution, Developments in Earth and Environmental Sciences. Elsevier, pp. 115–234.
- Davey, F., Brancolini, G., 1995. The Late Mesozoic and Cenozoic structural setting of the Ross Sea region. In: Cooper, A.K., Barker, P.F., Brancolini, G. (Eds.), Geology and Seismic Stratigraphy of the Antarctic Margin. Antarctic Research Series American Geophysical Union, pp. 167–182.
- De Santis, L., Anderson, J.B., Brancolini, G., Zayatz, I., 1995. Seismic record of late Oligocene through Miocene glaciation on the central and eastern continental shelf of the Ross Sea. In: Cooper, A.K., Barker, P.F., Brancolini, G. (Eds.), Geology and Seismic Stratigraphy of the Antarctic Margin. Antarctic Research Series American Geophysical Union, pp. 235–260.
- De Santis, L., Prato, S., Brancolini, G., Lovo, M., Torelli, L., 1999. The Eastern Ross Sea continental shelf during the Cenozoic: implications for the West Antarctic ice sheet development. *Glob. Planet. Chang.* 23, 173–196.
- De Santis, L., Brancolini, G., Donda, F., 2003. Seismo-stratigraphic analysis of the Wilkes Land continental margin (East Antarctica): influence of glacially driven processes on the Cenozoic deposition. *Deep Sea Res. Part II Top. Stud. Oceanogr.* 50, 1563–1594.
- DeConto, R.M., Pollard, D., 2016. Contribution of Antarctica to past and future sea-level rise. *Nature* 531, 591–597.
- Denton, G.H., Bockheim, J.G., Wilson, S.C., Stuiver, M., 1989. Late Wisconsin and early Holocene glacial history, inner Ross Embayment, Antarctica. *Quat. Res.* 31, 151–182.
- Donda, F., O'Brien, P., De Santis, L., Rebesco, M., Brancolini, G., 2008. Mass wasting processes in the Western Wilkes Land margin: possible implications for East Antarctic glacial history. *Palaeogeogr. Palaeoclimatol. Palaeoecol.* 260, 77–91.
- Dowdeswell, J.A., Cofaigh, C.Ó., Pudsey, C.J., 2004. Thickness and extent of the subglacial till layer beneath an Antarctic paleo-ice stream. *Geology* 32, 13–16.
- Escutia, C., Brinkhuis, H., Klaus, A., The Expedition 318 Scientists, 2011. Proceedings of the Integrated Ocean Drilling Program 318. Integrated Ocean Drilling Program Management International, Tokyo.
- Eyles, C., Eyles, N., 2010. Glacial deposits. In: James, N.P., Dalrymple, R.W. (Eds.), Facies Models 4, GEOText. The Geological Association of Canada, pp. 73–104.
- Faugères, J.-C., Stow, D.A., Imbert, P., Viana, A., 1999. Seismic features diagnostic of contourite drifts. *Mar. Geol.* 162, 1–38.
- García, M., Ercilla, G., Anderson, J.B., Alonso, B., 2008. New insights on the post-rift seismic stratigraphic architecture and sedimentary evolution of the Antarctic Peninsula margin (Central Bransfield Basin). *Mar. Geol.* 167–182.
- García, M., Hernández-Molina, F.J., Alonso, B., Vázquez, J.T., Ercilla, G., Llave, E., Casas, D., 2016. Erosive sub-circular depressions on the Guadalquivir Bank (Gulf of Cadiz): interaction between bottom current, mass-wasting and tectonic processes. In: Contourite Log-Book Significance Palaeoceanography Ecosyst. Slope Instab. 378. pp. 5–19.
- Gasson, E., DeConto, R.M., Pollard, D., Levy, R.H., 2016. Dynamic Antarctic ice sheet during the early to mid-Miocene. *Proc. Natl. Acad. Sci.* 113 (13), 3459–3464.
- Golledge, N.R., Levy, R.H., McKay, R.M., Fogwill, C.J., White, D.A., Graham, A.G., Smith, J.A., Hillenbrand, C.-D., Licht, K.J., Denton, G.H., Ackert Jr., R.P., Maas, S.M., Hall, B.L., 2013. Glaciology and geological signature of the Last Glacial Maximum Antarctic ice sheet. *Quat. Sci. Rev.* 78, 225–247.
- Golledge, N., Menzies, L., Carter, L., Fogwill, C., England, M., Cortese, G., Levy, R., 2014. Antarctic contribution to meltwater pulse 1A from reduced Southern Ocean overturning. *Nat. Commun.* 5.
- Granot, R., Cande, S., Stock, J., Davey, F., Clayton, R., 2010. Postspreading rifting in the Adare Basin, Antarctica: regional tectonic consequences. *Geochem. Geophys. Geosyst.* 11.
- Halberstadt, A.R.W., Simkins, L.M., Greenwood, S.L., Anderson, J.B., 2016. Past ice-sheet behaviour: retreat scenarios and changing controls in the Ross Sea, Antarctica. *Cryosphere* 10, 1003–1020.
- Haq, B.U., Hardenbol, J., Vail, P.R., 1987. Chronology of fluctuating sea levels since the Triassic. *Science* 235, 1156–1167.
- Harris, P.T., Macmillan-Lawler, M., Rupp, J., Baker, E.K., 2014. Geomorphology of the oceans. *Mar. Geol.* 352.
- Hayes, D., Frakes, L., 1975. General synthesis, deep sea drilling project leg 28. Initial Rep. Deep Sea Drill. Proj. 28, 919–942.
- Houtz, R., Davey, F., 1973. Seismic profiler and sonobuoy measurements in Ross Sea, Antarctica. *J. Geophys. Res.* 78, 3448–3468.
- Huang, X., Jokat, W., 2016. Middle Miocene to present sediment transport and deposits in the Southeastern Weddell Sea, Antarctica. *Glob. Planet. Change* 139, 211–225.
- Jacobs, S.S., Giulivi, C.F., Mele, P.A., 2002. Freshening of the Ross Sea during the late 20th century. *Nature* 297, 386–389.
- Laberg, J., Vorren, T., 1995. Late Weichselian submarine debris flow deposits on the Bear Island Trough mouth fan. *Mar. Geol.* 127, 45–72.
- Lee, J.I., McKay, R.M., Golledge, N.R., Yoon, H.I., Yoo, K.-C., Kim, H.J., Hong, J.K., 2017. Widespread persistence of expanded East Antarctic glaciers in the southwest Ross Sea during the last deglaciation. *Geology* 45, 403–406.
- Levy, R., Harwood, D., Florindo, F., Sangiorgi, F., Tripati, R., von Eynatten, H., Gasson, E., Kuhn, G., Tripati, A., DeConto, R., Fielding, C., Field, B., Golledge, N., McKay, R., Naish, T., Olney, M., Pollard, D., Schouten, S., Talarico, F., Warny, S., Willmott, V., Acton, G., Panter, K., Paulsen, T., Taviani, M., Science Team, S.M.S., 2016. Antarctic ice sheet sensitivity to atmospheric CO<sub>2</sub> variations in the early to mid-Miocene. *Proc. Natl. Acad. Sci.* 113 (13), 3453–3458.
- Lewis, A.R., Merchant, D.R., Ashworth, A.C., Hemming, S.R., Machlus, M.L., 2007. Major middle Miocene global climate change: evidence from East Antarctica and the Transantarctic Mountains. *Geol. Soc. Am. Bull.* 119, 1449–1461.
- Lewis, A.R., Merchant, D.R., Ashworth, A.C., Hedenäs, L., Hemming, S.R., Johnson, J.V., Leng, M.J., Machlus, M.L., Newton, A.E., Raine, J.I., Willenbring, J.K., Williams, M., Wolfe, A.P., 2008. Mid-Miocene cooling and the extinction of tundra in continental Antarctica. *Proc. Natl. Acad. Sci.* 105, 10676–10680.
- Lindeque, A., Gohl, K., Henrys, S., Wobbe, F., Davy, B., 2016. Seismic stratigraphy along the Amundsen Sea to Ross Sea continental rise: a cross-regional record of pre-glacial to glacial processes of the West Antarctic margin. *Palaeogeogr. Palaeoclimatol. Palaeoecol.* 443, 183–202.
- Livingstone, S.J., Cofaigh, C.Ó., Stokes, C.R., Hillenbrand, C.-D., Vieli, A., Jamieson, S.S., 2012. Antarctic paleo-ice streams. *Earth-Sci. Rev.* 111, 90–128.
- McKay, R., Browne, G., Carter, L., Cowan, E., Dunbar, G., Krissel, L., Naish, T., Powell, R., Reed, J., Talarico, F., Wilch, T., 2009. The stratigraphic signature of the late Cenozoic Antarctic Ice Sheets in the Ross Embayment. *Geol. Soc. Am. Bull.* 121, 1537–1561.
- McKay, R.M., Naish, T., Carter, L., Riesselman, C., Dunbar, R., Sjuneskog, C., Winter, D., Sangiorgi, F., Warren, C., Pagani, M., Schouten, S., Willmott, V., Levy, R., DeConto, R., Powell, R.D., 2012. Antarctic and Southern Ocean influences on Late Pliocene global cooling. *Proc. Natl. Acad. Sci.* 109, 6423–6428.
- McKay, R.M., Barrett, P.J., Levy, R.S., Naish, T.R., Golledge, N.R., Pyne, A., 2016. Antarctic Cenozoic climate history from sedimentary records: ANDRILL and beyond. *Philos. Trans. R. Soc. Lond. Math. Phys. Eng. Sci.* 374.
- McKay, R.M., De Santis, L., Kulhanek, D.K., 2017. Expedition 374 Scientific Prospectus: Ross Sea West Antarctic Ice Sheet History. International Ocean Discovery Program.
- Miramontes, E., Cattaneo, A., Jouet, G., Théreau, E., Thomas, Y., Rovere, M., Cauquil, E., Trincardi, F., 2016. The Pianosa Contourite Depositional System (Northern Tyrrhenian Sea): drift morphology and Plio-Quaternary stratigraphic evolution. In: Contourite Log-Book Significance Palaeoceanography Ecosyst. Slope Instab. 378. pp. 20–42.
- Mosala, A.B., Anderson, J.B., 2006. Expansion and rapid retreat of the West Antarctic Ice Sheet in eastern Ross Sea: possible consequence of over-extended ice streams? *Quat. Sci. Rev.* 25, 2177–2196.
- Mulder, T., 2011. Gravity processes and deposits on continental slope, rise and abyssal plains. In: Hüneke, H., Mulder, T. (Eds.), Deep-Sea Sediments. Elsevier, pp. 25–148.
- Naish, T., Powell, R., Barrett, P., Horgan, H., Dunbar, G., Wilson, G., Levy, R., Robinson, N., Carter, L., Pyne, A., Niessen, F., Bannister, S., Balfour, N., Damaske, D., Henrys, S., Kyle, P., Wilson, T., 2006. ANDRILL McMurdo Ice Shelf Project, Scientific Prospectus, ANDRILL Science Management Office, ANDRILL Contribution 4. University of Nebraska-Lincoln.
- Ó Cofaigh, C., Taylor, J., Dowdeswell, J.A., Pudsey, C.J., 2003. Palaeo-ice streams, trough mouth fans and high-latitude continental slope sedimentation. *Boreas* 32, 37–55.
- O'Grady, D.B., Syvitski, J.P., 2002. Large-scale morphology of Arctic continental slopes: the influence of sediment delivery on slope form. In: Dowdeswell, J.A., Ó Cofaigh, C. (Eds.), Glacier-Influenced Sedimentation on High-Latitude Continental Margins, Geological Society Special Publication. The Geological Society of London, pp. 11–32.
- Patterson, M., McKay, R., Naish, T., Escutia, C., Jimenez-Espejo, F., Raymo, M., Meyers, S., Tauxe, L., Brinkhuis, H., Expedition 318 Scientists, I.O.D.P., 2014. Orbital forcing of the East Antarctic ice sheet during the Pliocene and Early Pleistocene. *Nat. Geosci.* 7, 841–847.
- Pollard, D., DeConto, R.M., 2009. Modelling West Antarctic ice sheet growth and collapse through the past five million years. *Nature* 458, 329–332.

- Prather, B.E., 2003. Controls on reservoir distribution, architecture and stratigraphic trapping in slope settings. *Mar. Pet. Geol.* 20, 529–545.
- Rebesco, M., Larter, R.D., Camerlenghi, A., Barker, P.F., 1996. Giant sediment drifts on the continental rise west of the Antarctic Peninsula. *Geo-Mar. Lett.* 16, 65–75.
- Rebesco, M., Larter, R.D., Barker, P.F., Camerlenghi, A., Vanneste, L.E., 1997. The history of sedimentation on the continental rise west of the Antarctic Peninsula. In: Barker, P.F., Cooper, A.K. (Eds.), *Geology and Seismic Stratigraphy of the Antarctic Margin*, 2. Antarctic Research Series, vol. 71. AGU, pp. 29–49.
- Rebesco, M., Camerlenghi, A., Geletti, R., Canals, M., 2006. Margin architecture reveals the transition to the modern Antarctic ice sheet ca. 3 Ma. *Geology* 34, 301–304.
- Rebesco, M., Hernández-Molina, F.J., Van Rooij, D., Wählén, A., 2014. Contourites and associated sediments controlled by deep-water circulation processes: state-of-the-art and future considerations. *Mar. Geol.* 352, 111–154.
- Rignot, E., Mouginot, J., Scheuchl, B., 2011. Ice flow of the Antarctic ice sheet. *Science* 333, 1427–1430.
- Ryan, W.B., Carbotte, S.M., Coplan, J.O., O'Hara, S., Melkonian, A., Arko, R., Weissel, R.A., Ferrini, V., Goodwillie, A., Nitsche, F., Bonczkowski, J., Zemsky, R., 2009. Global multi-resolution topography synthesis. *Geochem. Geophys. Geosyst.* 10.
- Rydningen, T.A., Laberg, J.S., Kolstad, V., 2015. Seabed morphology and sedimentary processes on high-gradient trough mouth fans offshore Troms, northern Norway. *Geomorphology* 246, 205–219.
- Selvans, M.M., 2011. Geophysical Investigations of Near-Surface Structure on the Earth and Mars. California Institute of Technology.
- Selvans, M., Stock, J., Clayton, R., Cande, S., Granot, R., 2014. Deep crustal structure of the Adare and Northern Basins, Ross Sea, Antarctica, from sonobuoy data. *Earth Planet. Sci. Lett.* 405, 220–230.
- Shipp, S.S., Anderson, J., Domack, E., 1999. Late Pleistocene–Holocene retreat of the West Antarctic Ice-Sheet system in the Ross Sea: part 1—geophysical results. *Geol. Soc. Am. Bull.* 111, 1486–1516.
- Smith, W.O.J., Sedwick, P.N., Arrigo, K.R., Ainley, D.G., Orsi, A.H., 2012. The Ross Sea in a sea of change. *Oceanography* 25, 90–103.
- Stoker, M.S., Akhurst, M.C., Howe, J.A., Stow, D.A.V., 1998. Sediment drifts and contourites on the continental margin off northwest Britain. *Contourites Turbid. Process Interact.* 115, 33–51.
- Taylor, J., Dowdeswell, J.A., Kenyon, N.H., Ó Cofaigh, C., 2002. Late Quaternary architecture of trough-mouth fans: debris flows and suspended sediments on the Norwegian margin. In: Dowdeswell, J.A., Ó Cofaigh, C. (Eds.), *Glacier-Influenced Sedimentation on High-Latitude Continental Margins*, Geological Society Special Publication. The Geological Society of London, pp. 55–71.
- Uenzelmann-Neben, G., 2006. Depositional patterns at drift 7, Antarctic Peninsula: along-slope versus down-slope sediment transport as indicators for oceanic currents and climatic conditions. *Mar. Geol.* 233, 49–62.
- Uenzelmann-Neben, G., Gohl, K., 2012. Amundsen Sea sediment drifts: archives of modifications in oceanographic and climatic conditions. *Mar. Geol.* 299, 51–62.
- Veeken, P.C.H., van Moerkerken, B., 2013. *Seismic Stratigraphy and Depositional Facies Models*. EAGE publications. Academic Press.
- Vorren, T.O., Laberg, J.S., 1997. Trough mouth fans—palaeoclimate and ice-sheet monitors. *Quat. Sci. Rev.* 16, 865–881.
- Vorren, T., Lebesbye, E., Andreassen, K., Larsen, K.-B., 1989. Glacigenic sediments on a passive continental margin as exemplified by the Barents Sea. *Mar. Geol.* 85, 251–272.
- Wardell, N., Childs, J., Cooper, A., 2007. Advances through collaboration: sharing seismic reflection data via the Antarctic Seismic Data Library System for Cooperative Research (SDLS). In: *Antarctica: A Keystone in a Changing World—Online Proceedings for the 10th International Symposium on Antarctic Earth Sciences*, USGS Open-File Report 2007-1047. 001 (Short Research Paper).
- Wilson, D.S., Luyendyk, B.P., 2009. West Antarctic paleotopography estimated at the Eocene-Oligocene climate transition. *Geophys. Res. Lett.* 36 (L16302).
- Wilson, D.S., Jamieson, S.S.R., Barrett, P.J., Leitchenkov, G., Gohl, K., Larter, R.D., 2012. Antarctic topography at the Eocene-Oligocene boundary. *Palaeogeogr. Palaeoclimatol. Palaeoecol.* 335–336, 24–34.
- Winsborrow, M.C.M., Clark, C.D., Stokes, C.R., 2010. What controls the location of ice streams? *Earth-Sci. Rev.* 103, 45–59.
- Wright, R., Anderson, J.B., 1982. The importance of sediment gravity flow to sediment transport and sorting in a glacial marine environment: eastern Weddell Sea, Antarctica. *Geol. Soc. Am. Bull.* 93, 951–963.
- Wynn, R.B., Stow, D.A.V., 2002. Classification and characterisation of deep-water sediment waves. *Mar. Geol.* 192, 7–22.
- Yokoyama, Y., Anderson, J.B., Yamane, M., Simkins, L.M., Miyairi, Y., Yamazaki, T., Koizumi, M., Suga, H., Kusahara, K., Prothro, L., Hasumi, H., Southon, J.R., Ohkouchi, N., 2016. Widespread collapse of the Ross Ice Shelf during the late Holocene. *Proc. Natl. Acad. Sci.* 113, 2354–2359.
- Zachos, J., Pagani, M., Sloan, L., Thomas, E., Billups, K., 2001. Trends, rhythms, and aberrations in global climate 65 Ma to present. *Science* 292, 686–693.